AD-A226 855

CRREL REPORT 90-3

CRREL

Heat Transfer From Water Flowing Through a Chilled-Bed Open Channel

Paul W. Richmond and Virgil J. Lunardini

May 1990

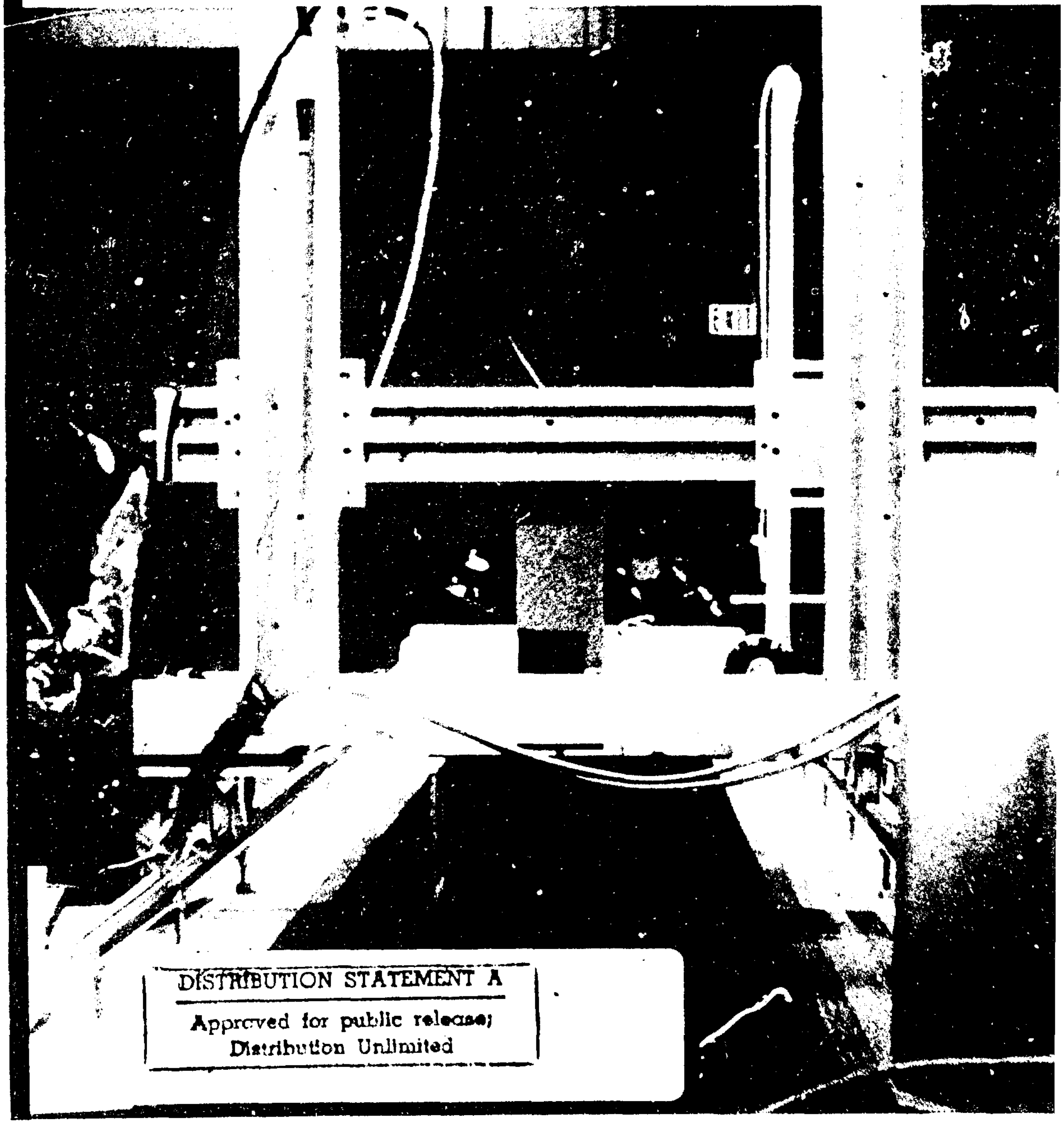

For conversion of SI metric units to U.S./British customary units of measurement consult ASTM Standard E380, Metric Practice Guide, *published by the American Society for Testing and Materials, 1916 Race St., Philadelphia, Pa. 19103.*

Cover: Narrow chilled-bed flume. (Photo by R. Demars.)

CRREL Report 90-3

U.S. Army Corps
of Engineers
Cold Regions Research &
Engineering Laboratory

Heat Transfer From Water Flowing Through a Chilled-Bed Open Channel

Paul W. Richmond and Virgil J. Lunardini

May 1990

Prepared for
OFFICE OF THE CHIEF OF ENGINEERS

PREFACE

This report was prepared by Paul W. Richmond and Dr. Virgil J. Lunardini, Mechanical Engineers, of the Applied Research Branch, Experimental Engineering Division, U.S. Army Cold Regions Research and Engineering Laboratory. This study was funded by DA Project 4A762730A4AL, *In-House Laboratory Independent Research.*

The authors express their appreciation to the people at CRREL who assisted in this project. Particular thanks go to Thomas Tantillo and Ronald Farr for construction of the flume, to James Morse for his help with the data acquisition system and to Michael Dunn who assisted in conducting the experiments.

The authors thank Dr. George Ashton, Dr. Horst Richter and Dr. Bengt Sonnerup for their technical review of this report.

CONTENTS

ILLUSTRATIONS

TABLES

Heat Transfer From Water Flowing Through a Chilled-Bed Open Channel

PAUL W. RICHMOND AND VIRGIL J. LUNARDINI

INTRODUCTION

The determination of heat transfer coefficients for water flowing over ice has been of interest for a number of years. Initially, research in this area developed from curiosity as to the cause of ripples on the underside of ice covers on frozen rivers and from the desire to predict ice cover growth and decay. Recently, work in this area has been conducted to obtain heat transfer correlations applicable to the use of large masses of ice for dissipating waste heat in self-contained, underground installations (Lunardini et al. 1986).

Observations have shown that the heat transfer is much greater for water flowing over ice than for water flowing over flat plates without melting. Early work in this area consisted of observations of the occurrence and behavior of wave shapes on the underside of river ice covers (Carey 1966, 1967, Larsen 1969, Ashton and Kennedy 1970, 1972). Following this work, a number of investigators (Gilpin et al. 1980, Ashton 1972, and Hsu et al. 1979) examined how these ripples are formed and their effect on the heat transfer coefficient. In these studies, heat transfer rates from initially plane ice surfaces were given limited analysis, the greater interest being in the formation of rippled ice. Hirata et al. (1979a and 1979b) examined steady-state melting of ice on plates in the entrance region, and confirmed that higher heat transfer rates occur than with plates without ice. In their turbulent regime work, where the concern was with the mechanism of transition, the heat transfer rate was also higher than predicted by flat plate theory. Haynes and Ashton (1979) presented new data for water flow in large aspect channels and compared their data with one analytical and one empirical model, without good agreement. Zisson (1984) conducted experiments in a large open-channel flume, studying the melting of horizontal bottom ice. These experiments were of short duration (7–8 hours) and average heat transfer rates were determined throughout the flow regime, including some natural convection experiments. Further analysis (Lunardini et al. 1986) of the data showed that for low flow rates and with the water temperatures above 3.4°C the heat transfer rate does not drop below the value for free convection (approximately 489 W/m^2). In general, they attributed the heat transfer rates greater than the nonmelting case to increased free stream turbulence, thermal instability due to the density inversion of water near 4°C and turbulent eddies associated with the generation of a wavy ice surface during melting, especially at high Reynolds numbers.

The present study was initiated in an attempt to further define the cause of increased heat transfer in water flowing over ice. The approach taken in this study was to eliminate some of the characteristics of melting ice such as turbulent eddy generation due to a wavy ice surface and flux of meltwater, while maintaining a similar temperature range. In order to accomplish this, a small open-channel flume was constructed for which the heat flow from the bed without the presence of ice could be measured. From these data it was anticipated that a more complete understanding of the heat transfer could be obtained.

BACKGROUND

Forced convection heat transfer correlations are generally presented as a relation between Reynolds number, Nusselt number and Prandtl number.

The Reynolds number, a ratio of viscous and inertia forces, is used to categorize flow. The definition of the Reynolds number is

$$\mathrm{Re} = \frac{VL}{\nu_f} \tag{1}$$

where Re = Reynolds number
V = mean fluid velocity
ν_f = kinematic viscosity of the fluid at the film or bulk temperature
L = characteristic length.

Two characteristic lengths can be used in correlating heat transfer data for the horizontal flat surfaces of a flume. These are the length from the flow inlet to the point of interest, and the hydraulic diameter, defined as four times the flow area divided by the wetted perimeter. This definition of hydraulic diameter is standard for heat transfer correlations and is four times the value often used in hydraulics.

The Nusselt number is defined as

$$\mathrm{Nu} = \frac{hL}{k_f} \tag{2}$$

where h is the convective heat transfer coefficient and k_f is the thermal conductivity of the fluid.

The Prandtl number is the ratio of the diffusion of momentum to the diffusion of energy, in a fluid, and characterizes the relative growths of the momentum and thermal boundary layers. The definition is

$$\mathrm{Pr} = \frac{\nu_f}{\alpha_f} \tag{3}$$

where ν_f and α_f are the kinematic viscosity and thermal diffusivity, respectively.

Although these terms were defined by material properties evaluated at the film temperature, they can also be defined using properties based on the bulk flow temperature. Bulk flow properties are generally used in specifying internal flow while film temperatures are typically used when describing external flows. This convention is used in later analyses.

The data obtained in these experiments were for the flow of water in an open channel with turbulent flow. The Reynolds numbers (based on hydraulic diameter) extended from fully turbulent values through Reynolds numbers generally described as the transition region values. Bulk water temperatures ranged from 5° to 33°C and channel bed surface temperatures ranged from near zero to about 9°C. In order to determine the effect of the density inversion on the heat transfer coefficient, data were collected for bed surface temperatures below 4°C and were compared with data collected at bed temperatures above 4°C. It was expected that the data obtained with the bed temperature below 4°C would compare well with those for flow over melting ice. Similarly, the data obtained with higher bed temperatures should compare well with standard heat transfer correlations. Heat transfer correlations for melting ice and for water at low temperatures are limited. The majority of the correlations for water exist for internal flow at temperatures above 4°C.

For data obtained in an open channel, the first type of correlation that one is tempted to consider is that of semi-infinite flow over a flat plate. This is an external flow configuration and the characteristic length is taken as the distance from the leading edge of the plate. This flow is developing (as opposed to being fully developed); that is, the momentum or velocity and thermal boundary layers have not reached their maximum thicknesses. The Von Karman analogy (Von Karman 1939) is widely used for turbulent flow, where the fluid properties are based on the film temperatures and the subscript x refers to entrance length:

$$Nu_x = \frac{0.0292\ \mathrm{Pr}\ \mathrm{Re}_x^{0.8}}{1 + \frac{0.855}{\mathrm{Re}_x^{0.1}}\{\mathrm{Pr} - 1 + \ln\ [1 + 5/6\ (\mathrm{Pr} - 1)]\}} . \tag{4}$$

Gilpin et al. (1980) conducted an experiment with ice on a flat plate and developed a correlation, based on boundary layer thickness, which Lunardini et al. (1986) converted to a correlation based on entrance length, for comparison purposes

$$Nu_x = 0.00284\ \mathrm{Pr}\ \mathrm{Re}_x^{0.888} \qquad (\mathrm{Pr} \approx 13). \tag{5}$$

For laminar flow, Chapman (1967) suggests

$$Nu_x = 0.332\ \mathrm{Re}_x^{1/2}\ \ \mathrm{Pr}^{1/3} . \tag{6}$$

The velocity profile above a flat plate is considered two-dimensional, while that of the open channel is three-dimensional. The data presented in this report were obtained at the centerline of the channel, and from this point of view it may be acceptable to compare the data with these correlations. However, a more significant difference lies in the comparison of fully developed vs developing flow, and for this reason the use of the entrance length as a parameter is given only limited analysis. Later in this report it is shown that for these experiments the flow was fully developed.

Correlations obtained from analysis of tube flow are more appropriate for comparison to open-channel flow than the flat plate correlations because of the greater similarity between velocity profiles. Vanoni (1941) demonstrated that the Prandtl logarithmic velocity distribution law for tube flow also applies to infinitely wide open channels. For turbulent, fully developed flow the following equations are often used. The McAdams (1940) equation for circular pipe flow is

$$Nu_D = 0.023\ \mathrm{Pr}^{0.3}\ \mathrm{Re}_D^{0.8} . \tag{7}$$

The subscript D refers to the use of the pipe diameter as the characteristic length. For noncircular tubes the hydraulic diameter (H) is often substituted. The equation is similar to the Dittus-Boelter equation (Eckert and Drake 1959):

$$Nu = 0.0243\ \ \mathrm{Re}_D^{0.8}\ \ \mathrm{Pr}^{0.4}, \ \text{for heating} \tag{8a}$$

$$Nu = 0.0265\ \ \mathrm{Re}_D^{0.8}\ \ \mathrm{Pr}^{0.3}, \ \text{for cooling} . \tag{8b}$$

Petukov and Popov (1963) suggest

$$Nu_D = \frac{\mathrm{Re}_D\,\mathrm{Pr}\ (C_f/2)}{1.07 + 12.7\ (\mathrm{Pr}^{2/3} - 1)\sqrt{C_f/2}} \tag{9}$$

where $C_f/2 = (2.236\ \ln \mathrm{Re}_D - 4.639)^{-2}$.

Sieder and Tate's (1936) correlation is

$$Nu_D = 0.027\ \mathrm{Re}_D^{0.8}\ \mathrm{Pr}^{0.33}\left(\frac{\mu}{\mu_{surface}}\right)^{0.14} \tag{10}$$

where μ is the dynamic viscosity, and the material properties are based on the bulk temperature rather than the film temperature. For fully developed laminar flow in tubes, Hausen (1943) suggests

$$Nu_D = 3.66 + \frac{0.0668\,(D/L)\,Re_D Pr}{1 + 0.04\left[(D/L)\,Re_D Pr\right]^{2/3}} \tag{11}$$

where D and L are the pipe diameter and length, respectively. The limiting Nusselt value for fully developed laminar flow in circular tubes is about 3.66. The Reynolds numbers for the transition region are generally taken as between 2000 and 10,000 (based on hydraulic diameter).

Clearly, the best comparisons of the data would be expected with correlations developed from open-channel experiments. However, there are few of these correlations available. Ashton and Kennedy (1972) correlated their data based on water depth d for water flowing over ice in an open-channel flume,

$$Nu_d = 0.078\ Re_d^{0.8} \qquad (Pr \approx 13). \tag{12}$$

Since the width of the flume was 0.61 m, rewriting eq 12 in terms of hydraulic diameter yields

$$Nu_H = 0.078\ Re_H^{0.8}\ (0.61 + 2d)^{-0.2}\ . \tag{13}$$

Lunardini et al. (1986) correlated their open-channel flow data for water flowing over ice as

$$Nu_H = 0.0078\ Pr^{1/3}\ Re_H^{0.927}\ . \tag{14}$$

EXPERIMENTAL APPARATUS

In order to obtain heat transfer data without ice that could be compared with melting correlations, an experiment was conducted to investigate mechanisms that affect heat transfer to water flowing over a chilled channel bed. A small experimental flume was designed and constructed in which heat transfer coefficients of fully established flow could be measured and observed.

Flume

A 15.2-m-long by 30.48-cm-wide recirculating open-channel flume was constructed in the Frost Effects Research Facility (FERF) of the U.S. Army Cold Regions Research and Engineering Laboratory. The flume was assembled primarily from plywood coated with fiberglass epoxy resin, while the bed was fabricated from ALCOA type 300 precision cast tool and jig aluminum plate. Large pass, Platecoil heat transfer panels were installed under the entire length of the aluminum bed. Heat transfer mastic (Tracit no. 1000) was used to ensure a continuous bond between the panels and the bed. Figure 1 shows a cross section of the flume. The head and tail boxes are approximately 0.37 m^2. Wire mesh and "horsehair" packaging material were used initially to reduce turbulence of the water entering the flume and a small turning vane was placed in the entrance to the tail box in order to reduce air entrainment in the

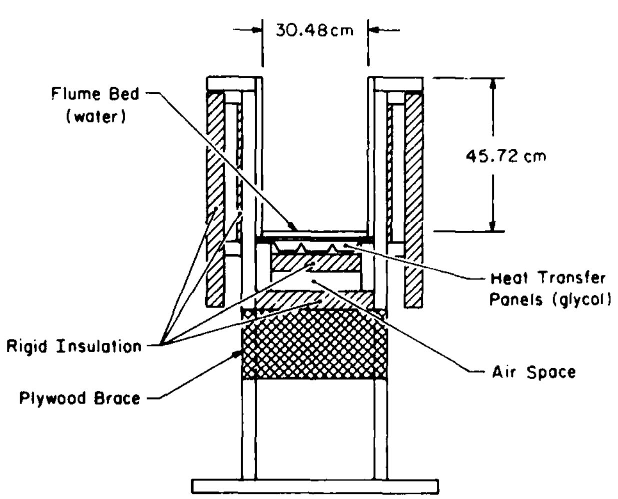

Figure 1. Cross section of flume.

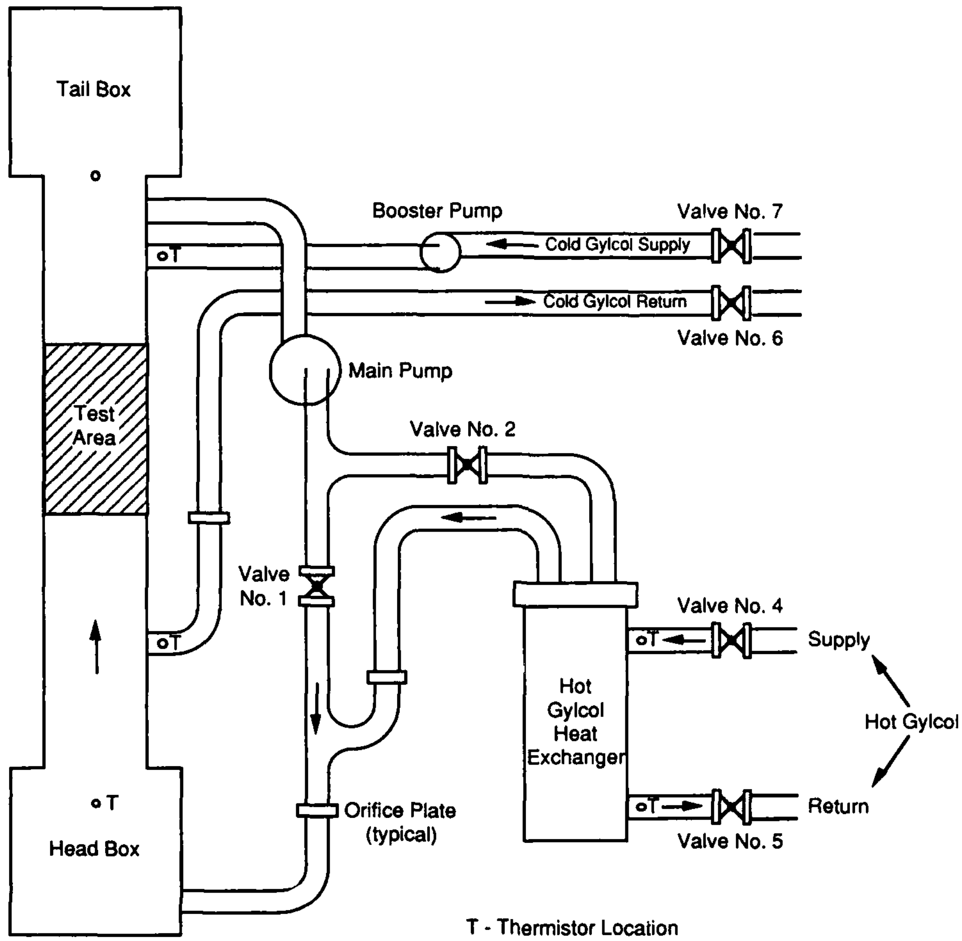

Figure 2. Schematic diagram of flume.

water at low flow depths. The sides and bottom of the flume were insulated with Styrofoam insulation.

The design parameters of the flume were developed from several criteria. A relatively small flume was desired for economic reasons and a smaller flume was expected to allow greater control of experimental parameters. The desire to drill holes in the edge of the flume bed for installation of thermistors at the centerline of the flume limited its width because longer drill bits would tend to drift excessively and cause sensor misplacement or break through the surface. Once the width was determined, other parameters were developed based on the desire for fully developed turbulent flow. Construction of the flume and installation of the instrumentation took about 6 months, with the majority of that time spent on interfacing and programing the various instrumentation components.

Figure 2 shows a schematic diagram of the flume and associated pumps, valves and flow meters. The main pump was rated at 5.6 kW (7.5 hp) and was capable of pumping $3.15 \times 10^{-2} m^3/s$ (500 gpm) of water through the flume. A heat exchanger located after the pump discharge and in parallel with the main piping could be used to control the temperature of the water entering the flume. Warm glycol was pumped through this heat exchanger by pump no. 11 ($2.5 \times 10^{-3} m^3/s$ at 413 kPa, 40 gpm at 60 psi) of the FERF. Cold glycol was pumped through the heat transfer panels located under the flume bed by pump no. 12 ($2.5 \times 10^{-3} m^3/s$ at 413 kPa, 40 gpm at 60 psi) and a booster pump (1.1 kW, 1.5 hp) which was installed in the glycol supply line.

Orifice plates were installed as indicated in Figure 2 and Tygon tubing was used to construct manometers, from which flow rates were determined manually. The manometer calibration curves are included in Richmond (1988).

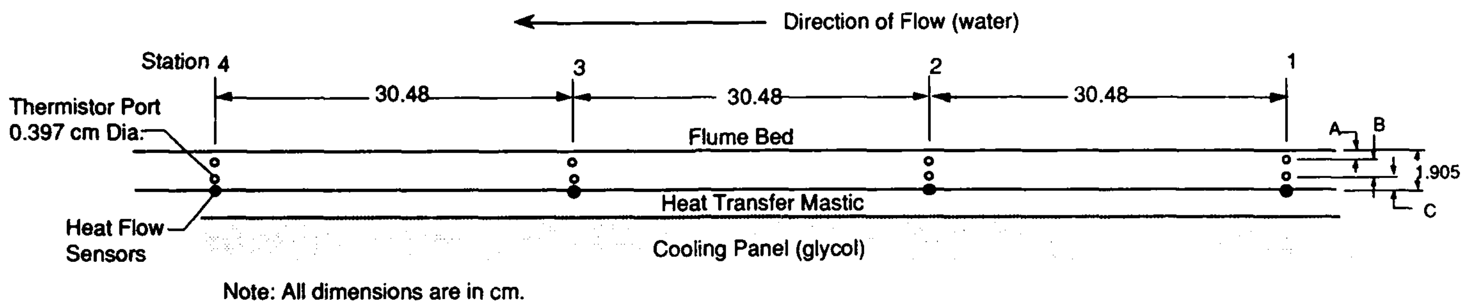

Station *Dimension (cm)*	*1*	*2*	*3*	*4*
A	0.3048	0.3255	0.3175	0.3205
B	1.2827	1.262	1.27	1.267
C	0.3175	0.3175	0.3175	0.3175
Distance from flume entrance (m)	10.55	10.86	11.16	11.46

Figure 3. Test section detail.

An area approximately 10 m from the entrance was designated the test section. This 1.5-m-long section was constructed slightly differently from the other parts of the flume, in that here the walls were made of 1.9-cm-(0.75-in.) thick clear plexiglass. Additionally, in this section holes were drilled into the edge of the aluminum bed such that thermistors could be embedded along the centerline (Fig. 3). By knowing the distance between the thermistors, the temperatures and the thermal conductivity of the aluminum plate, one could calculate the heat flow through the bed. During assembly, in order to obtain another measure of heat flow, heat flow sensors (Micro-Foil, from RdF Corporation, 20453-1 SP), which had a thermocouple built into the plastic mount, were epoxied onto the underside of the flume bed along the centerline, and below the thermistors (Fig. 3).

Thermistors were installed at each of the locations indicated in Figure 2 in order to obtain fluid temperatures. For the thermistors installed within pipes, thermistor wells were constructed from 0.3175-cm (1/8-in.) copper tubing by pinching and soldering one end of the tubing; the tubing was then bent so that the tube would be well into the flow. The tubing was then installed within the pipe and the pipe hole sealed around the tubing. All the thermistors installed in cavities were coated with Dow 340 heat sink compound.

Table 1. Sensor nomenclature.

Sensor type	*Location description*	*Accuracy*[1]
Thermistor[2]	≈0.32 cm below bed surface at stations 1–4	0.02°C
Thermistor	≈1.58 cm below bed surface at stations 1–4	0.02°C
Heat flow[3]	Epoxied to underside of bed at stations 1–4	—
Thermocouple	Epoxied to underside of bed at stations 1–4	0.1°C
Thermocouple[4]	Temperature/velocity probe Hot film anemometer[5]	0.04°C —
Thermistor	Water inlet, heat exchanger	0.02°C
Thermistor	Water outlet, heat exchanger	0.02°C
Thermistor	Air temperature	0.02°C
Thermistor	Flume exit, 3 cm below water surface	0.02°C
Thermistor	Glycol exit below flume bed	0.02°C
Thermistor	Glycol entrance	0.02°C
Thermistor	Flume entrance, in head box	0.02°C
LVDT[6]	Carriage location	0.15 cm
LVDT[7]	Ice depth	—

[1]Estimated
[2]Victory Engineering Corp., model T32A11, 2000 ohm
[3]RdF 20453-1 Heat flow sensor w/thermocouple
[4]28 gauge copper-constantan
[5]TSI hot film sensor
[6]Celesco PT 101-60A, 60-in. position transducer
[7]Schaevitz HPD 3000, 3-in. position transducer

Data acquisition

The data acquisition system evolved as information was required and associated instrumentation was acquired. Ideally, all of the following data would be collected at the same instant:

1. Heat flow through the bed
2. Vertical temperature profile in the water
3. Vertical velocity profile in the water
4. Ice surface profile along the length of the test section in the direction of flow (if ice was present)
5. Water depth and flow rates
6. Water and glycol temperatures

From these data a number of parameters were to be calculated, in particular the Nusselt, Prandtl and Reynolds numbers.

Data acquisition equipment

The data acquisition components used in these experiments are described in Tables 1 and 2. Figure 4 shows a schematic of the data acquisition system. In this instrumentation assembly, an HP-85 microcomputer served as the system controller, a built-in printer allowed hard copy data output of system temperatures and flow characteristics between tests, and a larger external printer was used to produce a hard copy of the test data. Thermistor resistance readings were made and converted to digital signals by the multiplexer (as were voltage outputs from the linear voltage displacement transducers [LVDT], thermocouples and heat flow sensors). The data were then acquired by the HP-85.

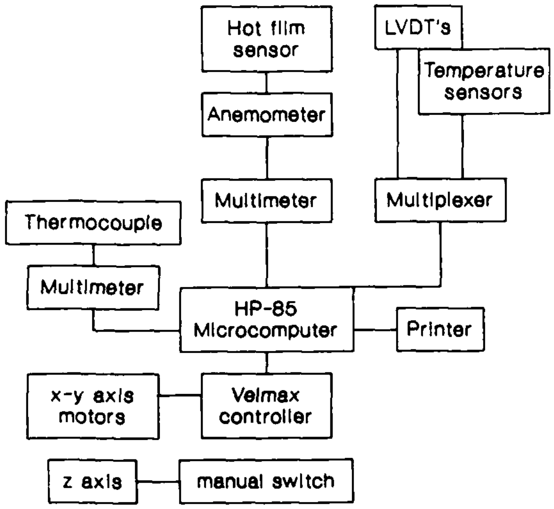

Figure 4. Data acquisition system.

Table 2. Data acquisition hardware.

Nomenclature	*Use*
1. HP*-85A computer, 32-kbyte	Data acquisition controller memory, HP-IB and RS232-C interfaces.
2. HP 3124A multiplexer w/ 5 1/2 digit multimeter	To make thermistor, heat flow sensor, LVDT, and thermocouple readings
3. 2 HP 34784 multimeters	Monitor velocity sensor and attached thermocouple
4. Model 8300 series Velmax motor control, RS 232-C compatible	Allows HP-85 to control probe location
5. HP Thinkjet Printer	Test data printout

*HP—Hewlett-Packard

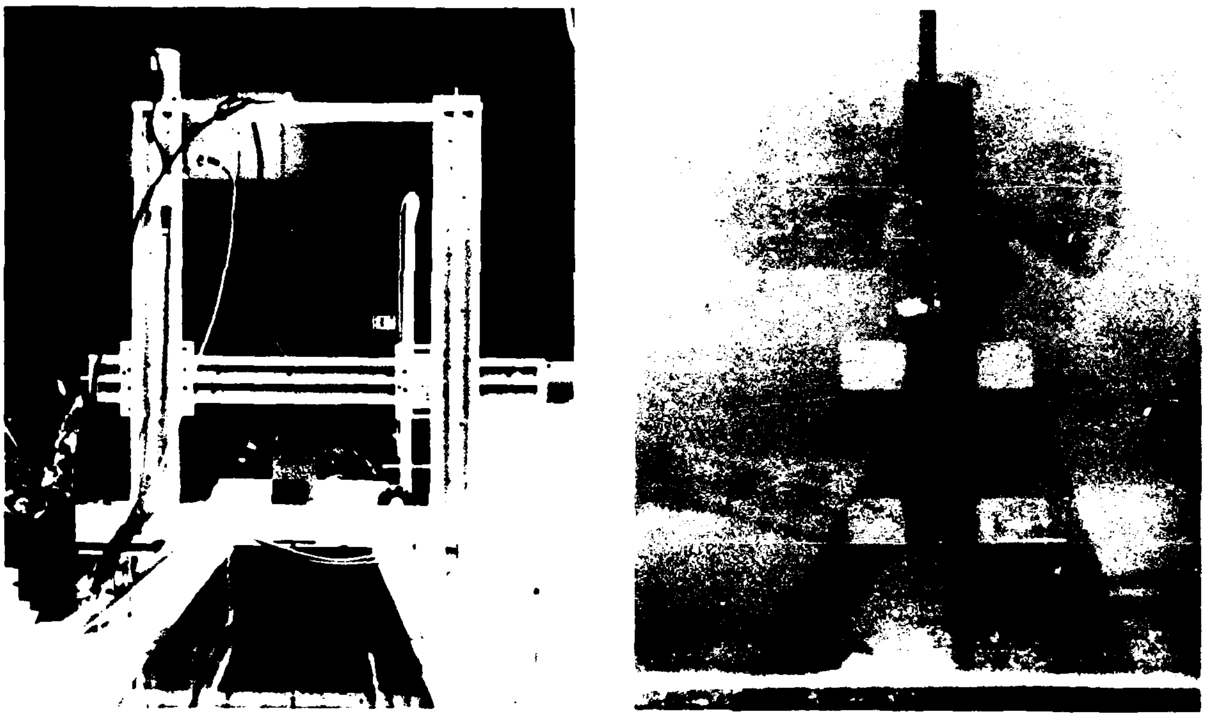

a. Probe mounted on carriage. *b. Underwater view of sensors.*

Figure 5. Hot film/thermocouple probe.

An x–y carriage assembly supported a combination hot-film sensor and 28-gauge copper-constantan thermocouple probe (Fig. 5). The x–y coordinates of the probe were controlled by the HP-85 computer via the Velmax motor controller. Outputs from these two sensors were input to the HP-85 via two HP-4784 multimeters (which could be read by the HP-85 faster than from the multiplexer). Velocity measurements were to have been made with hot film sensors and a TSI model 1050 constant temperature anemometer.

An LVDT could be attached in place of the hot film/thermocouple sensor in order to profile the ice thickness when present. If an ice profile test were to be run, the z axis (horizontal and parallel to the flow) DC motor would be turned on manually and the LVDT used to determine the ice thickness.

Software

A data acquisition program was written for the HP-85 computer which allowed it to communicate with the peripheral devices listed in Table 2. The program converted voltage and resistance measurements to appropriate units, displayed or printed the data, and then stored the test data on magnetic data cassette tape. Figure 6 presents a flowchart of the data acquisition program. A copy of the program is included as Appendix A. From Figure 6 it can be seen that after the program is started a menu appears which asks what type of data is to be obtained.

The five choices are 1) monitor any thermistor channel, 2) monitor system, 3) conduct temperature/velocity profile test, 4) measure ice profile, and 5) exit program. The selection of "monitor any thermistor channel" (1) allows the user to select a desired thermistor, the number of readings to be made and the time lapse between readings. The resistance readings are converted to temperatures and then printed on the internal printer. "Monitor system" (2) takes readings of the thermistors, heat flow sensors, and thermocouples, and then does some preliminary analysis. Typical output of this routine is shown in Figure 7. The temperature/velocity profile test routine (4) operates similarly to "monitor system" (2) except that at each station measurements from the velocity/temperature probe are made. The program asks the user for the number of vertical positions (in the flow) and the increment or distance between readings. The number of horizontal (perpendicular or transverse to the flow) positions is entered along with the distance from the centerline (+ or –) for each transverse position, and the vertical locations are repeated at each transverse position. At the end of the measurement section of this routine, basic data are recorded on the magnetic tape cassette. The data then are printed

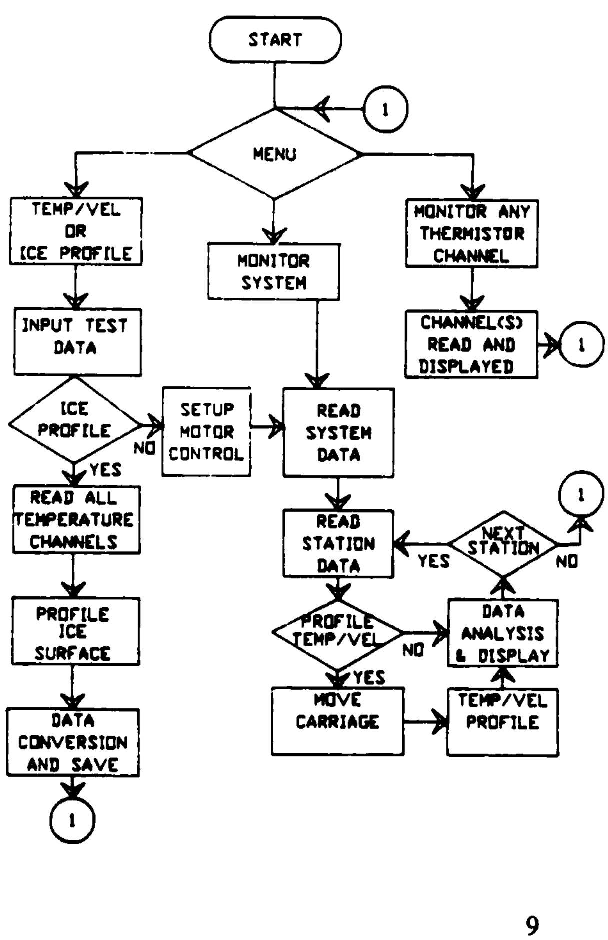

Figure 6. Flow chart of data acquisition program.

on the external printer along with the results of the initial data analysis (heat flow values, Reynolds number, Nusselt number, etc.). Appendix B contains a typical output from this routine. The "monitor" routines (1 and 2) were used to determine when the system had reached a steady state.

The ice profile routine allowed periodic measurements of an ice thickness on the flume bed and allowed up to 150 ice thickness measurements to be made over the 1.2-m test section. Due to time constraints experiments with ice present were not conducted; hence this routine was never used and no ice melting data were collected.

Calibration and accuracy

Table 1, as previously noted, contains the nomenclature for each of the sensors used in collecting data. This section of the report will describe how the output of these sensors was converted to the desired units and the associated accuracy. This section also discusses how other values needed to complete the data analysis were obtained.

Temperature data were obtained from two types of sensors, thermistors and thermocouples. The thermistors were obtained with calibration data at –40°C, 0°C and 25°C, the resistance measurements were specified at ± 0.01% and the temperature at ± 0.01°C. These data were then fitted to the Steinhart-Hart equation (Stanley 1967), which was then used to convert the resistance measurement to temperature:

```
TIME 11 4125797222
AIR TEMP  18.98
FLUME ENTRANCE TEMP   4.23
FLUME EXIT TEMP   4.21
COLD GLYCOL ENTR -33.59
COLD GLYCOL EXIT -32.09
HOT GLYCOL ENTR  14.73
HOT GLYCOL EXIT  14.74

STATION  1
HEAT FLOW METER -352.887
HEAT FLOW X PLATE (.55)-1606 284
TEMP AT BOTTOM OF PLATE-1.64
THERMISTER AT BOTTOM      .50
THERMISTER AT TOP        .65
CALC PLATE SURF     .69

STATION  2
HEAT FLOW METER -184.294
HEAT FLOW X PLATE (.55)-2821 184
TEMP AT BOTTOM OF PLATE-.385
THERMISTER AT BOTTOM    1.09
THERMISTER AT TOP     1 35
CALC PLATE SURF   1.42

STATION  3
HEAT FLOW METER -235.175
HEAT FLOW X PLATE (.55)-3043.040
TEMP AT BOTTOM OF PLATE-1.491
THERMISTER AT BOTTOM      .89
THERMISTER AT TOP     1.17
CALC PLATE SURF   1.24

STATION  4
HEAT FLOW METER -184.335
HEAT FLOW X PLATE (.55)-3124.355
TEMP AT BOTTOM OF PLATE-.478
THERMISTER AT BOTTOM      .92
THERMISTER AT TOP     1.20
CALC PLATE SURF   1.28
```

Figure 7. Typical output of "system monitor."

$$\frac{1}{T} = A + B \ln R + C (\ln R)^3 \tag{15}$$

where T = temperature in kelvins
R = resistance of the thermistor
A, B, C = curve fit constants

In order to make accurate measurements from thermistors it is necessary to have a low current flow to avoid self-heating. With the HP-3421A this was accomplished by using the 300 kilo-ohm resistance range (10–μA current) during the measurements which provided a measurement accuracy of ± 0.00315% of reading + 3 counts, in ohms. Counts refer to the value of the last place in the reading. The accuracy of a 2000-ohm resistance would be 3.06 ohms, with the HP-3421A at room temperature. This corresponds to about ±0.02°C for measurements in the 0° to 25°C range. At ambient temperatures different from about 23°C, slightly higher inaccuracies are possible. The thermocouples used were copper-constantan and the thermocouples connected to the heat flow sensors had an accuracy of ± 0.1°C when used with the HP-3421A. The thermocouple used to measure the water temperature profiles was constructed from 28-gauge thermocouple wires, carefully welded together and then coated with insulating varnish. This thermocouple was calibrated using a thermistor as a reference, with each placed in a constant temperature ethanol bath. The reference junction for the thermocouple circuit was placed in an ice bath. A new ice bath was made at the beginning of each day. A straight line was fitted to the resulting temperature–voltage data (Fig. 8); the accuracy of this thermocouple was estimated to be 0.04°C.

The heat flow sensors were obtained with individual calibration data from the manufacturer, and no additional calibration was done. At 21°C the sensors utilized were to have an output of 6.3442

$\mu V/W\text{-}m^{-2}$ ($0.02\ \mu V/BTU\text{-}ft^{-2}\text{-}hr^{-1}$) and a curve to correct for different temperatures was also provided. The output from the multiplexer was in volts; therefore, division of the output voltage by the calibration constant and multiplication by the temperature factor should have yielded a measure of heat flow. However, this was not the case, and these sensors did not yield any reasonable data. The only possible explanation for this was that the epoxy used to adhere these sensors to the bottom of the plate was acting as an insulator. This was supported by the thermocouple output that tended to be lower than anticipated for the bottom surface of the aluminum plate, making up the flume bed.

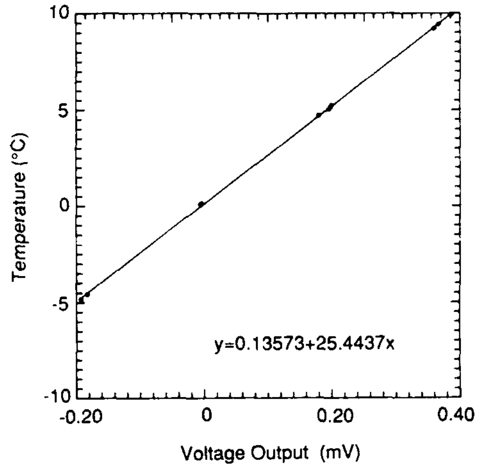

Figure 8. Thermocouple calibration curve.

The constant temperature anemometer was obtained under a rental contract with TSI Inc. A water probe calibrator was also obtained from TSI with the anticipation that frequent recalibration of the sensors would be required. The flume was designed and constructed without capability for filtering the water, as we thought that if the water became too dirty it could be drained and the flume refilled with clean water. Cheese cloth was placed over a screen at the entrance and used as a coarse filter. (Other tests that were being done in the FERF created a dusty environment and for this reason the flume was kept covered with plastic sheets which minimized dust settlement into the water.) It was anticipated that dirt in the water would have some effect on the hot film sensors, and discussions with a TSI representative indicated that the buildup of dirt would be gradual and probably could be accommodated with frequent calibrations. This was not the case and no reliable data were obtained. The addition of a diatomaceous earth filter did not improve the hot film sensor data.

Since the anemometer did not provide acceptable flow velocity data, it was necessary to determine the mean flow velocity from the orifice plates by making manual measurements of the difference in fluid height in the manometers. Of primary concern was the orifice plate located in the head box supply line. Two different manometers were constructed: a manometer for high flow rates that contained mercury and a lower flow rate manometer that used water. Calibration curves were produced for each manometer and it was estimated that the accuracy obtained from these measurements would be $\pm 3.15 \times 10\ m^{-4}/s$ (5 gpm). This flow rate was converted to the mean water velocity by using the principle of conservation of mass.

The cross-sectional area of the flume occupied by the flow was determined by reading the water depth at each test station from a scale taped to the plexiglass. This depth measurement was accurate to within 0.1 cm. The water depth was multiplied by 30.48 cm to obtain the area. Flow depths ranged from 10 to 30 cm, so the inaccuracy of this measurement was about $\pm$ 1% in the worst case.

In order to determine the heat flux through the flume bed two additional values were required, the distance between the thermistors within the plate and the conductivity of the flume bed material. A value of 138 W/m K for the conductivity of the aluminum was obtained from the manufacturer's specification data (ALCOA). An attempt was also made to obtain the conductivity using CRREL's guarded hot plate apparatus; however, no usable value was obtained due to difficulties in using this method with high conductivity materials. It was therefore estimated that the conductivity was accurate to 10% and that this would include any effect of the thermistor glass and the heat sink compound around the thermistors. The holes were drilled into the edge of the plate as near to the surface as possible without risking breaking through the surface. The distance from the surface to the holes was later checked with an ultrasound device. The average distance between the thermistors was determined to be 0.0127 m $\pm$ 0.0001 m; the individual measurements for each test station were used in calculating the heat flux (Fig. 3).

EXPERIMENTAL PROCEDURE AND CONDITIONS

As mentioned earlier in this report, data were collected only for no-ice conditions. Data were collected after the system had reached a steady state, identified by little or no change in the temperature observations made using the system monitor subprogram. For high flow rate experiments, steady state could be obtained in one to two hours, while with lower flow rates it could take 8 hours or more to obtain the desired conditions. Generally, two complete sets of data were recorded in quick succession in order to obtain eight data points under nearly the same conditions.

In tests conducted before the water filter was obtained, the flume was rinsed out and refilled with fresh water prior to testing each day. After a filter was obtained, the bed was wiped down and the filter turned on. With valves 1 and 2 (Fig. 2) shut off, the main pump was turned on. Valves 1 and 2 were then gradually opened, and water was added continually until it was at the desired depth. The water depth was generally between 10 and 15 cm except for some low flow tests where the depth was as high as 31 cm. At this point the manometer lines were purged of air by manipulation of tubing clamps. The glycol valves (4–6) were left open, pumps 11 and 12 were turned on, and the temperature of the glycol in these lines adjusted. The glycol temperatures ranged between –37° and –2°C for the cooling panels. Some experimentation was done in an attempt to maximize heat flow into the glycol from the flume bed; thus a flow rate of $2.08 \times 10^{-3} m^3/s$ at –33°C was generally used. The warm glycol for the heat exchanger was generally set at 12°C and adjusted as needed. The bulk water temperature of the flume was maintained by diverting some of the water through the warm glycol heat exchanger. The x–y carriage assembly was moved manually so that the hot film sensor probe was 1 mm (measured with a "feeler" gauge) above the plate surface centerline. The motor assembly, when turned on, accepted this position as zero in the transverse (perpendicular to flow) and vertical directions.

The experimental parameters considered the most important were the flow rate (Reynolds number) and bed surface temperatures. Since most of the tests were run at the same water depth and similar bulk water temperatures, the Reynolds number was varied by adjusting the flow rate. The flow rate through the flume was controlled by valves 1 and 2, and these were adjusted to maintain the desired flow rate and the temperature of the water. The water temperature was adjusted so that the plate surface temperature would be in the desired range.

Temperatures were monitored using the system monitor subroutine as described earlier. Additionally, if the flume bed temperature dropped below 0°C, ice could be observed on the flume bed through the plexiglass walls of the test section. The water temperature was lowered until ice began to form and then raised slightly. Adjustments were made as the flume came to equilibrium. The flume was assumed to be at a steady-state condition when the monitored temperatures ceased changing or were changing very slowly and randomly.

Four flow conditions were of interest for these experiments: turbulent flow with the plate surface temperature (T_s) near 0°C, turbulent flow with the plate surface above 4°C, and transitional flow (turbulent to laminar) with T_s near 0°C and above 4°C. For the transitional or low flow tests, the water-filled manometer was used in place of the mercury-filled manometer, allowing more accurate low flow rate measurements. Additionally, lower flow rates (less than $6.31 \times 10^{-3} m^3/s$ [100 gpm]) required warmer cold glycol temperatures or higher bulk water temperatures in order to prevent ice from forming on the flume bed.

RESULTS AND DATA ANALYSIS

Data were collected under the flow conditions described in the previous section, and Table 3 presents a summary of the data. Entry numbers refer to the test data obtained at each station, and are referenced to the data presented in Appendix C, which were compiled from the data acquisition system output. From the compiled data, Nusselt number vs Reynolds number correlations were obtained based on hydraulic diameter and on entrance length. These calculated parameters, along with the calculated heat flux, are also listed in Appendix C, and are cross-referenced by entry number to the complete set of data (Richmond 1988) which are too voluminous to include here. The data in Appendix C were sorted into the four flow conditions described in Table 3.

Table 3. Data summary.

Flow condition	*Plate surface temperature*	*Entry nos.*	*Average Prandtl no.**
Turbulent	>4°C	1–69, 232–259	9.3
	<4°C	70–183	10.1
Transition (turbulent to laminar)	<4°C	184–215	5.1
	>4°C	216–231	5.3

* Based on bulk temperatures.

In order to check that the momentum boundary layer was indeed fully developed at the test section, the fully established flow length was calculated for various flow rates. It was assumed that the flow was fully developed when the boundary thickness was the same as the water depth. Using the equation for flow over a flat plate (Schlichting 1955),

$$\delta = 0.37\, L \left(\frac{U_\infty \ell}{\nu}\right)^{-1/5} \tag{16}$$

for the turbulent boundary layer thickness, where U_∞ is the free stream velocity, the following distances to attain established flow (ℓ) were obtained:

Flow rate (GPM)	*Water depth δ (m)*	*Established* flow length (m)*
100	0.15	5.81
300	0.15	7.70
500	0.15	8.69

*Water temperature of 10°C.

The distance from the inlet to the test section was approximately 10 m, thus confirming that the flow was fully developed.

Figure 9 presents the Nusselt number vs Reynolds number data based on hydraulic diameter. The turbulent data are typical of those obtained for tubes; however, there is extensive scattering of the data in the transition region. The data obtained by Lunardini et al. (1986), with ice, for low Reynolds numbers, fall in the box shown in this figure.

The turbulent data for $T_s < 4°C$ begins at a Reynolds number of approximately 2×10^4 and that for $T_s > 4°C$ at about 3.5×10^4. From this observation it appears that the configuration with $T_s < 4°C$ is less stable than that with $T_s > 4°C$. This is consistent with earlier observations suggesting that melting cases ($T_s = 0°$) have convective instabilities. The low Reynolds number data seem to be scattered around the typical laminar/transition region for nonmelting systems rather than Lunardini's melting data, as might have been expected (based on temperature and density comparisons). The scatter in this region was caused by two problems. First, it was found during calibration of the system that cold spots existed along the flume bed; these cold spots were generally located near joints in the heat transfer panels. In these areas higher glycol flow rates existed within the panels, which subsequently caused higher heat fluxes in these same areas. Calculations showed that flow in the individual heat exchanger channels was laminar; thus heat transfer was limited. A small booster pump was added to the glycol supply line, but this did not completely solve the problem. For this reason different surface temperatures were obtained at each station. This difference varied from 0.2°C to 1.0°C. A significant problem with the data in the low Reynolds number region is inaccuracy. Poor accuracy in the calculated values (Nusselt, Reynolds number and heat flux) was caused by the small differences in the temperatures measured within the flume bed. An error analysis was done following Holman (1971),

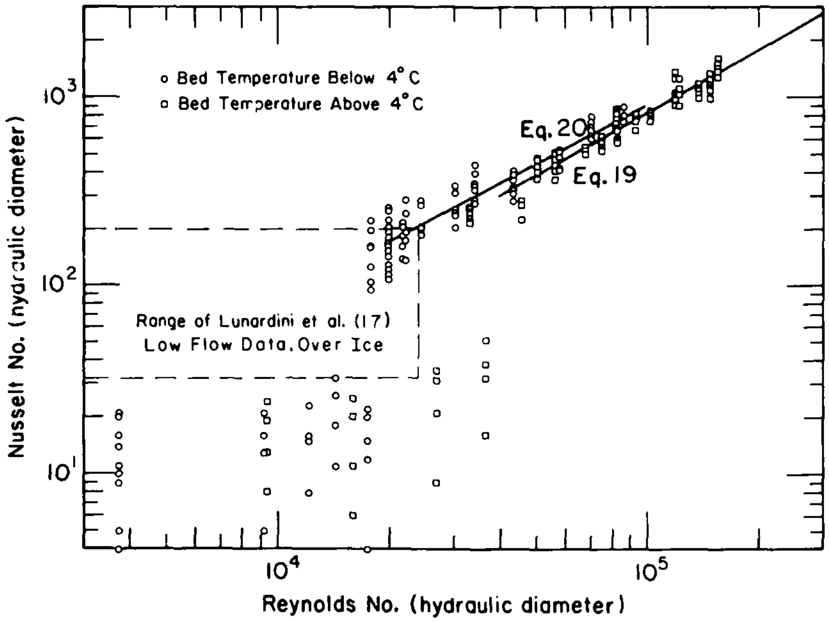

Figure 9. Nusselt number vs Reynolds number (hydraulic diameter).

where the uncertainty in a function R is defined by W_r and is calculated from uncertainties (W_n) in the independent variables X_1, X_2, X_3 ..., X_n as follows:

$$W_r = \left[\left(\frac{\partial R}{\partial X_1} W_1\right)^2 + \left(\frac{\partial R}{\partial X_2} W_2\right)^2 + \left(\frac{\partial R}{\partial X_3} W_3\right)^2 + \ldots\right]^{1/2}. \tag{17}$$

Using this equation (App. D), the equations for Nusselt number, Reynolds number and the uncertainties described above resulted in Figure 10, which shows graphically the potential error for various data points. The largest source of potential error was found to be due to small temperature differences between the thermistors embedded in the flume bed.

This problem had been anticipated during design of the flume, but was not resolved due to compromises to obtain low surface temperatures at higher flow rates. If the data had been in the range of the low flow test data of Lunardini et al. (1986), the potential error in the Nusselt number would have been more tolerable. This can be illustrated by calculating the maximum error associated with the heat flux determination due to measurement inaccuracy in the temperature alone. The error of the thermistors was ± 0.02°C; calculating the flux based on a temperature difference of 0.04°C (the maximum error associated with the temperature difference) yields 435 W/m^2. Comparing this value with the average measured value of the low flow rate heat flux (880 W/m^2 for T_s > 4°C) it can be

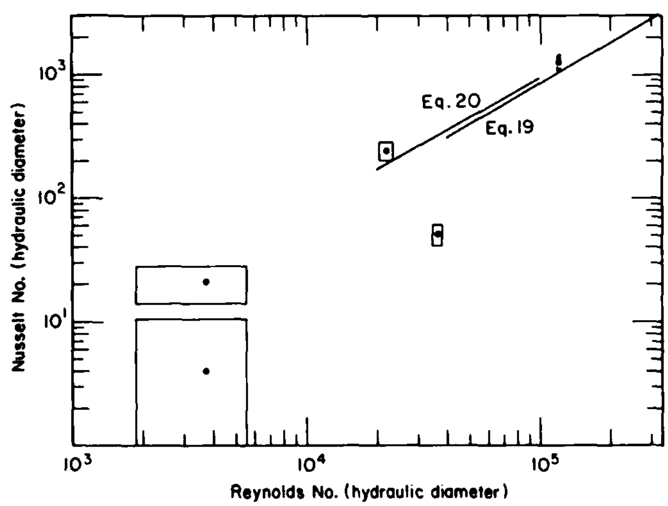

Figure 10. Maximum potential error in selected data points.

seen that the maximum error is close to 50% at these flow rates. It can be realized that as the heat flux increases the relative error is reduced. This large error in the low flow rate data makes the quantitative values of limited value and they are not included in any further analysis.

Heat transfer correlations of the turbulent data in Figure 9 were developed using a least-squares regression analysis. The equations were developed in the form of

$$\frac{\mathrm{Nu}}{\mathrm{Pr}^{1/3}} = A\ \mathrm{Re}^{B} \tag{18}$$

The use of the Prandtl number to the 1/3 power comes from observation of other correlations rather than any clear trend in the data. The correlations obtained for the turbulent region are

$$\frac{\mathrm{Nu_H}}{\mathrm{Pr}^{1/3}} = 0.00128\ \mathrm{Re_H^{1.096}} \qquad T_s > 4\,^\circ\mathrm{C} \quad 3 \times 10^4 < \mathrm{Re} < 1.5 \times 10^5 \tag{19}$$

$$\frac{\mathrm{Nu_H}}{\mathrm{Pr}^{1/3}} = 0.00265\ \mathrm{Re_H^{1.040}} \qquad T_s < 4\,^\circ\mathrm{C} \quad 1.5 \times 10^4 < \mathrm{Re} < 1.5 \times 10^5 \tag{20}$$

where T_s is the plate surface temperature. It can be seen from these equations that a higher (on the order of 10%) heat transfer rate is obtained for $T_s < 4°C$ than for $T_s > 4°C$. This is as anticipated from observations of melting systems, which inherently include the density inversion. These equations are plotted in Figure 9 and 10 using a Prandtl number of 10, and bulk flow temperature properties.

The data are also shown in Figure 11, with parameters based on entrance length and fluid properties based on film temperature. In Figure 11 it can be seen that the transition from laminar to turbulent flow occurs at about $\mathrm{Re_L} \approx 10^6$ as expected. It was established earlier that the flow was fully established and the data are presented in this form only for completeness. The correlations obtained were

$$\frac{\mathrm{Nu_x}}{\mathrm{Pr}^{1/3}} = 0.001366\ \mathrm{Re_x^{1.071}} \qquad T_s > 4\,^\circ\mathrm{C} \tag{21}$$

$$\frac{\mathrm{Nu_x}}{\mathrm{Pr}^{1/3}} = 0.00539\ \mathrm{Re_x^{0.9837}} \qquad T_s < 4\,^\circ\mathrm{C} \tag{22}$$

Returning to the analysis based on hydraulic diameter, Figure 12 compares eq 19 and 20 with some of the correlations discussed earlier.

Examination of Figure 12 shows that at low Reynolds numbers there is, in general, good agreement between all the correlations except that of McAdams (1940, eq 7). Both eq 13 (Ashton and Kennedy 1972) and eq 14 (Lunardini et al. 1986) compare very well with eq 9 (Petukov and Popov 1963). At higher Reynolds numbers, the equations (eq 19 and 20) obtained from the test data tend to diverge from the other correlations.

A number of possible explanations for this behavior are now examined.

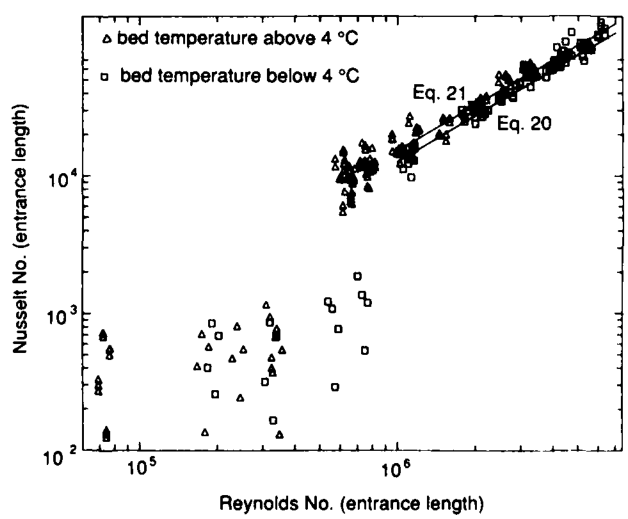

Figure 11. Nusselt number vs Reynolds number (entrance length).

During the experiments, it was thought that this might be caused by excess turbulence induced by unsettled entrance conditions, and because of this, a different turbulence-reducing mechanism was installed (hand-made aluminum grid flow straighteners). The results of additional tests (entries 232–259) did not significantly differ from earlier tests. The varying flume bed surface temperature could have had an effect on the turbulence in the boundary layer, but at higher flow rates (i.e., higher Reynolds numbers) this effect would be reduced.

Recalling that duct correlations may only agree with wide shallow channels and also noting that for most of the tests the width to depth ratio was about two, it is possible that the divergence may be caused by a velocity profile effect. Considering that this effect would be more pronounced at high Reynolds numbers supports this reasoning. The other open-channel correlations were obtained from relatively wide shallow flumes (width/depth = 7).

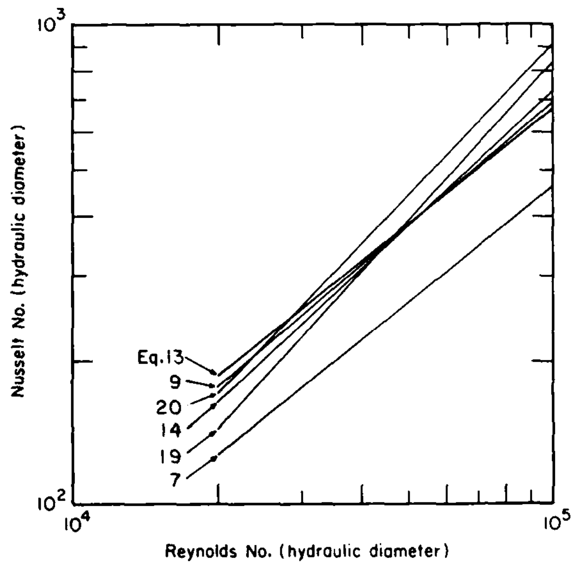

Figure 12. Comparison of heat transfer correlations (Prandtl number = 10).

Further literature review of the velocity distribution in narrow open channels vs wide channels confirmed that the velocity distribution in an open channel is dependent on the relative magnitude of channel width and depth (Rouse 1938). Since the velocity gradient at the boundaries will vary from point to point in a cross section, then the intensity of the boundary shear cannot be assumed constant over the walls and bed of the channel. A procedure presented by Vanoni (1977) provides a means of determining the average shear stress on the bed. This is accomplished by separating the shear force exerted on the bed from that on the walls. A bed shear velocity is then determined from which a corrected mean velocity can be obtained.

The procedure followed was to first determine the friction factor (f) for the flume. During initial tests of the flume and data acquisition system, Manning's friction coefficient (n) was found to be about 0.012. The friction factor is calculated from

$$f = 8g\left(\frac{n}{1.49}\right)^2 R^{-1/3} \tag{23}$$

where g is the acceleration due to gravity and R is the hydraulic radius (area/wetted perimeter). The value Re_H/f was then computed. A linear regression analysis was used to fit a curve to data points obtained from Vanoni's (1977) plot which related Re_H/f to f_w (friction factor associated with the walls). The equation developed was

$$f_w = 0.253\ (Re_H/f)^{-0.169}\ . \tag{24}$$

Once f_w was obtained, the friction factor due to the bed (f_b) was calculated using

$$f_b = f + \frac{2d}{b}(f - f_w) \tag{25}$$

where d is the water depth and b is the bed width. Continuing with Vanoni's procedure, the bed shear velocity (u_{*b}) was then calculated using

$$u_{*b} = \sqrt{gR_bS} = \frac{f_b\, v_{avg}^2}{8} \tag{26}$$

where v_{avg} is obtained from the mass flux, S is the shear stress and R_b is the bed hydraulic radius. The mean velocity at the centerline was then obtained from an equation presented by Yalin (1977), which relates the mean velocity to the bed shear velocity:

$$v = 2.5\, u_{*b} \ln \left(3.32\ \mathrm{Re}_{*b}\right) \tag{27}$$

where Re_{*b} is the Reynolds number based on the water depth and the bed shear velocity.

Since the procedure is intended to correct velocities in narrow flumes, application of the procedure to wider flumes, such as that used by Lunardini et al. (1986), should have little or no effect on the mean velocity. The results of calculations to check this hypothesis are shown below:

Reynolds number	*% change in velocity Narrow flume (0.3048 m)**	*Wide flume (1.2 m)+*
1.1615×10^5	25%	4.6%
3.4846×10^4	29%	8.5%

* Width/depth ≈ 2.
+ Width/depth ≈ 7.

As can be seen, there is only a small effect on the velocity in the wider flume at the higher flow rate, while at lower flow rates some effect is observed.

Appendix C contains Re_H values calculated using the velocity correction procedure. This velocity correction procedure is applicable only to the turbulent flow data, and of course only affected the Reynolds number calculations. The corrected data are plotted in Figure 13. Least-squares regression of this data resulted in the following set of equations:

$$\mathrm{Nu_H} = 0.006\ \mathrm{Pr}^{1/3}\ \mathrm{Re_H^{0.93}} \qquad T_s > 4\,°\mathrm{C} \tag{28}$$

$$\mathrm{Nu_H} = 0.0142\ \mathrm{Pr}^{1/3}\ \mathrm{Re_H^{0.864}} \qquad T_s < 4\,°\mathrm{C}. \tag{29}$$

The regression coefficients (r^2) were 0.95 and 0.88 for eq 28 and 29, respectively. Figure 14 presents the 95% confidence intervals for the two regressions; these intervals only begin to overlap at the upper limit of the $T_s < 4°\mathrm{C}$ data, i.e., $\mathrm{Re_H} \approx 1.1 \times 10^6$. It may be inferred from this analysis that the two regressions represent the influence of two different heat transfer phenomena.

The only obvious difference between these two data sets is T_s, which is below 4°C for eq 29, and which produces the higher heat transfer rate. In Figure 13 these equations are compared with some of the correlations presented earlier. Equation 29, which should correspond to the melting correlations, falls slightly below those correlations (eq 13 and 14). Two possible reasons for this difference are that 1) other heat transfer mechanisms are occurring in the case of melting and are enhancing the density inversion effect or 2) the average plate surface temperature was about 2.0°C as opposed to 0°C in the melting case. Pursuing this second possibility, we attempted to correlate the parameter $\mathrm{Nu_H}/(\mathrm{Pr}^{1/3}\mathrm{Re_H^{0.93}})$ with the plate surface temperature. In Figure 15, the above parameter is plotted against the difference between 4°C and the surface temperature; a least-squares regression line is fit to the data. Despite the considerable scatter of the data there is some indication that the surface temperature (when below 4°C) is related to the increased heat transfer observed in the correlation. The regression line nearly intersects the 0.6 value (from eq 28) at $T_s = 4$ and the 0.78 value (from eq 14, for melting ice) at $T_s = 0$ as might be expected.

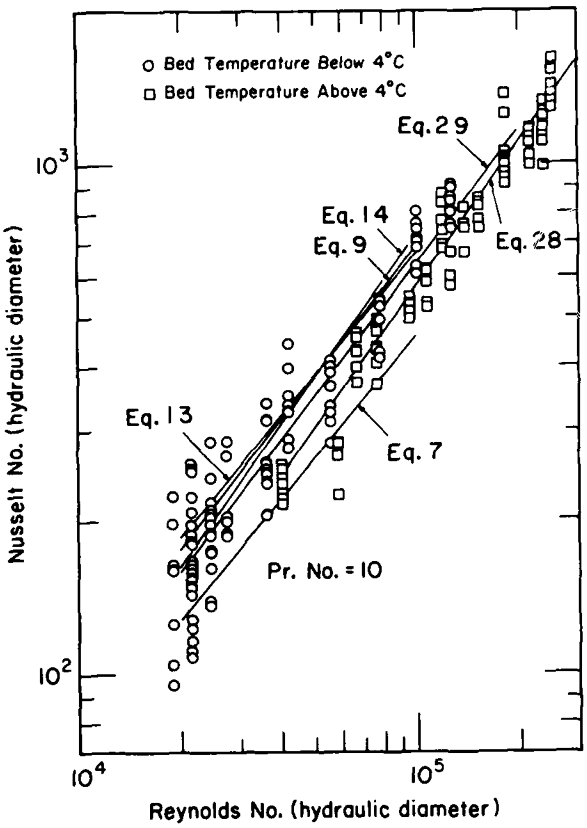

Figure 13. Nusselt number vs Reynolds number using the velocity correction.

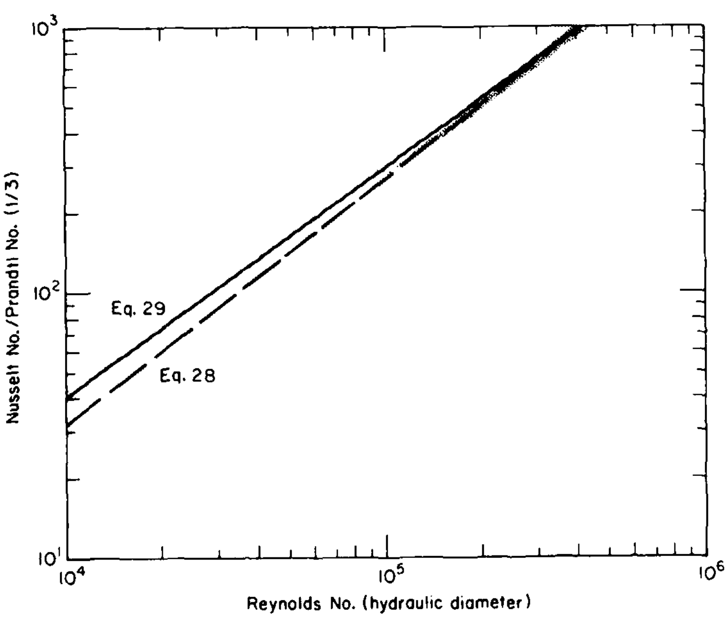

Figure 14. 95% confidence intervals for eq 28 and 29.

In regard to the comparison of eq 29 with eq 14 (for melting ice), other flow characteristics may be responsible for the increased heat transfer indicated by eq 14. Lunardini et al. (1986) suggested that other effects could be the flux of meltwater injected at the ice/water interface and increased free stream turbulence due to inherent waviness of a melting ice sheet.

Gilpin et al. (1978) conducted experiments in which the boundary layer temperatures were measured in a developing flow of water over heated and cooled plates. They observed similar convec-

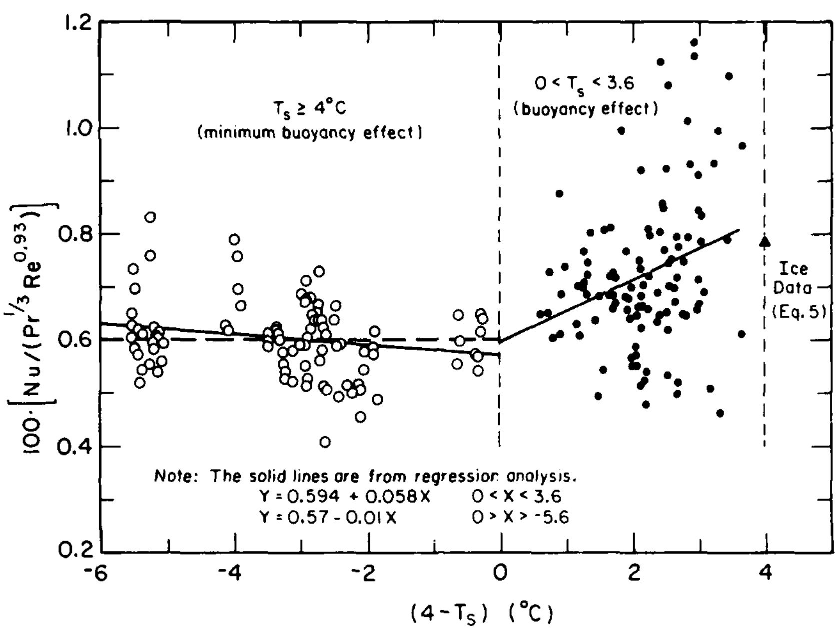

Figure 15. Effect of surface temperature on the correlation parameter.

tive instabilities in both cases and, for the case where the density maximum was present, a roughly constant temperature (4°C) for much of the boundary layer thickness was observed.

The significance of the work presented here is that the density inversion and subsequent instabilities may in part explain the increased heat transfer between melting and nonmelting systems observed in fully developed turbulent flow.

It should be noted that the difference between eq 28 and 29 is 15% at a Reynolds number of 5×10^4 and decreases at higher Reynolds numbers, suggesting a reduced effect of the density inversion as the Reynolds number increases. This is not supported by eq 14 (Lunardini et al. 1986); however, it is supported by eq 13 (Ashton and Kennedy 1972) and eq 9 (Petukov and Popov 1963). It seems plausible after examining the bed surface temperatures in Appendix C that this may also result because only relatively warm surface temperatures were obtainable at the higher Reynolds number (thus skewing the data).

In reference to Figure 13 once again, the difference between eq 28 and 7 (McAdams 1940) may be attributed to inherent differences between open-channel flow with cooling from the bed as compared with pipe flow with axisymmetric cooling. It is interesting to note that eq 28 has nearly the same exponent as eq 14 (0.927) obtained by Lunardini et al. (1986).

Figure 16 examines the correlations at Prandtl numbers other than 10, and it should be emphasized here that eq 13 (Ashton and Kennedy 1972) was based on a Prandtl number of 13 and is not a variable in their equation. Trends similar to those observed with a Prandtl number of 10 are observed; however, this may not be significant due to the limited Prandtl number data.

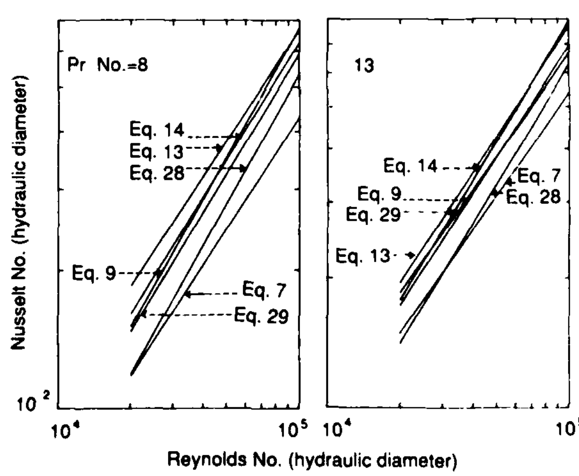

Figure 16. Comparison of correlations at other Prandtl numbers.

Lunardini et al. (1986) observed a relationship between the heat flux and Reynolds number for water flowing over melting ice at low flow rates (Re_H < 10,000). They observed a limiting heat flux of 488.5 W/m^2. This phenomenon is examined in Figure 17. Noting that only the turbulent data uses the velocity correction, it is seen that the low Reynolds number data are scattered around the value of 488.5 W/m^2, albeit with more scatter than shown by Lunardini et al. (1986). It is interesting to note that even with the plate temperature above 4°C (T_s > 4°C) the low flow data scattered around this same value.

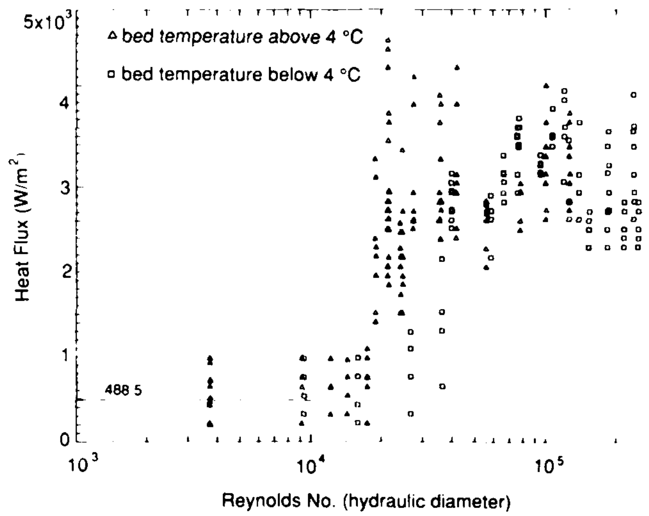

Figure 17. Heat flux vs Reynolds number (with velocity correction).

Comparison of the Nusselt numbers obtained for the low flow conditions with T_s > 4°C and T_s < 4°C indicates that there is no effect of the plate surface temperature on the heat transfer rate. This is the opposite of what is expected based on the data of Lunardini et al. (1986) and the turbulent flow data of these experiments. Lunardini et al. (1986) reported an average Nusselt number of 75; in these experiments an average value of 14 was found for flow in the same Reynolds number region. Several differences exist between the two experiments; in Lunardini et al. (1986) ice was present, the bulk temperature was on the order of 8°C and the water depth was about 0.25 m. In the experiments reported here, no ice was present, the bulk temperature was about 30°C and the water depth was about 0.25 m. Since the lack of ice did not significantly affect comparisons for the turbulent flow case, it is assumed that this is not the reason for the differences observed between the low flow rate data of the two experiments. The remaining difference is the temperature profile.

In the case of free convection, for enclosed horizontal layers, a critical layer thickness must be exceeded before the heat transfer rate can be enhanced by buoyancy effects. This value is generally described by the Rayleigh number and the critical value is 1700. The Rayleigh number is defined by

$$\mathrm{Ra} = \frac{\mathrm{Pr}\ g\beta\Delta T L^3}{\nu_f^2} \tag{30}$$

where g is the acceleration due to gravity, β is the thermal coefficient of expansion, ΔT is the temperature difference, and L is a characteristic length. Using this equation, with Ra set to 1700 and the upper and lower layer temperatures set at 4°C and 0°C respectively, yields a critical thickness of about 7 mm. Layer thicknesses less then 7 mm will act as conductive layers (Nu = 1), while for thicker layers, Bernard cells will develop and enhance heat transfer.

A possible reason for the increased heat transfer observed by Lunardini et al. (1986) could be the larger distance between the 0° and 4°C isotherms compared to the data of this report. A review of the temperature profiles for these data in Richmond (1988) showed that in all cases the 4°C isotherm was less than 1 mm thick. The temperature profile data of Lunardini et al. (1986) have not been published. Gilpin et al. (1978) examined the external flow case of flow developing on a flat horizontal plate, with the density inversion of water present, and were able to visualize an unstable region of vortex rolls between the 0° and 4°C isotherms. These ideas seem to explain the apparent differences between the two sets of open-channel data.

SUMMARY

A small cross-sectional area flume was constructed in which both the bed and entrance temperatures could be controlled. The flume was designed so that thermistors installed in the bed allowed the heat flux across the bed to be measured. Flow rates up to $3.15 \times 10^{-2} m^3/s$ (500 gpm) were possible. Flow velocities were determined from manometers measuring flow in the supply pipes, and a velocity correction procedure was used to compensate for the narrow flume. Experiments were conducted with Reynolds numbers based on hydraulic diameter up to 2.3×10^5. The flume had several limitations. It was not possible to measure small heat fluxes across the flume bed due to difficulties in obtaining temperatures with accuracies greater than 0.02°C, and uneven, limited cooling of the flume bed reduced its usefulness at high flow rates. These limitations mainly affected the accuracy of the Nusselt and Reynolds numbers at low flow rates as indicated in Figure 10, thus limiting the quantitative usefulness of the low flow rate data.

A slightly different heat transfer correlation was obtained for the flume as compared to that associated with pipe flow, which must be due to differences in the boundary conditions between the chilled-bed flume and axisymmetric pipe cooling.

Comparison of the two heat transfer correlations (eq 28 and 29) obtained from these experiments showed that an increase in heat transfer occurs when the plate surface temperature is below 4°C, which could be due to the density inversion of water at 4°C and subsequent flow instability. The heat transfer rate appears to be a function of 4°C minus the plate surface temperature, which supports the above conclusion that, as the plate temperature decreases below 4°C, the heat transfer is enhanced by the increasing buoyancy effect of the density inversion.

Extending these findings to comparisons of the correlations obtained by others from water flowing over melting ice indicates that the density inversion of water plays an important role in the increased heat transfer rate in fully developed turbulent flow, although other effects are not ruled out. Other researchers, (e.g., Gilpin et al. 1978) have shown that cooling is similar to heating over a flat plate if the density maximum exists; that is, if the plate surface temperature is below 4°C in the entrance region. This work demonstrates that the instabilities continue into the fully developed flow regime and explains in part the increased heat transfer observed in fully developed melting systems.

LITERATURE CITED

Ashton, G.D. (1972) Field implications of the formation of ice ripples. *In Proceedings of IAHR Symposium: Ice and its Action on Hydraulic Structures, 26–29 Sept., Leningrad, USSR.* International Association for Hydraulic Research, p. 123–129.

Ashton, G.D. and J.F. Kennedy (1970) Temperature and flow conditions during the formation of river ice. *In Proceedings of IAHR Symposium: Ice and Its Action on Hydraulic Structures, Reykjavik, Iceland.* International Association for Hydraulic Research, paper no. 2.4.

Ashton, G.D. and J.F. Kennedy (1972) Ripples on the underside of river ice covers. *Journal of the Hydraulics Division, Proceedings of the American Society of Civil Engineers,* **98**(HY9): 1603–1624.

Carey, K.L. (1966) Observed configuration and computed roughness of the underside of river ice, St. Croix River, Wisconsin. U.S. Geological Survey Professional Paper 550-B, p. B192–B198.

Carey, K.L. (1967) The underside of river ice, St. Croix River, Wisconsin. U.S. Geological Survey Prof. Paper 575-C, p. C195–C199.

Chapman, A.J. (1967) *Heat Transfer.* New York: MacMillan.

Eckert, E.R.G. and R.M. Drake (1959) *Heat and Mass Transfer.* New York: McGraw-Hill.

Gilpin, R.R., T. Hirata and D.C. Cheng (1978) Longitudinal vortices in a horizontal boundary layer in water including the effects of the density maximum at 4°C. American Society of Mechanical Engineers paper 78-HT-25.

Gilpin, R.R., T. Hirata and D.C. Cheng (1980) Wave formation and heat transfer at an ice–water interface in the presence of turbulent flow. *Journal of Fluid Mechanics*, **99**(3): 619–640.

Hausen, H. (1943) Darstellung des Warmeuberganges an Rohren durch Verallgemeinerte Potenzbeziehungen. Zeitschr. V.D.I. Beihefte Verfahrenstechnik, No. 4, p. 91.

Haynes, F.D. and G.D. Ashton (1979) Turbulent heat transfer in large aspect channels. USA Cold Regions Research and Engineering Laboratory, CRREL Report 79-13.

Hirata, T., R.R. Gilpin, K.C. Cheng and E.M. Gates (1979a) The steady state ice layer profile on a constant temperature plate in a forced convection flow—I. Laminar regime. *International Journal of Heat and Mass Transfer*, **22**: 1425–1433.

Hirata, T., R.R. Gilpin and K.C. Cheng (1979b) The steady state ice layer profile on a constant temperature plate in a forced convection flow—II. The transition and turbulent regimes. *International Journal of Heat and Mass Transfer*, **22**: 1435–1443.

Holman, J.P. (1971) *Experimental Methods for Engineers*. New York: McGraw-Hill.

Hsu, K.S., F.A. Locher and J.F. Kennedy (1979) Forced-convection heat transfer from irregular melting wavy boundaries. *Journal of Heat Transfer*, Nov. 1979, p. 598–602.

Larsen, P.A. (1969) Head losses caused by an ice cover on open channels. *Journal of the Boston Society of Civil Engineers*, **56**(1): 45–67.

Lunardini, V. J., J. R. Zisson and Y. C. Yen (1986) Heat transfer coefficients in water flowing over a horizontal ice sheet. USA Cold Regions Research and Engineering Laboratory, CRREL Report 86-3.

McAdams, W.H. (1940) Review and summary of developments in heat transfer by conduction and convection. *Transactions, American Institute of Chemical Engineers*, **36**(1).

Petukov, B.S. and V.N. Popov (1963) Theoretical calculation of heat exchange and frictional resistance in turbulent flow in tubes of an incompressible fluid with variable physical properties. Moscow Energetics Institute, *Teplofizika Vysokikh Temperatur*, **1**(1).

Richmond, P.W. (1988) Temperature and flow data. Water over a chilled flume bed. USA Cold Regions Research and Engineering Laboratory, Internal Report 1018 (unpublished).

Rouse, H. (1938) *Fluid Mechanics for Hydraulic Engineers*. New York: McGraw-Hill.

Savino, J.M. and R. Siegel (1967) Experimental and analytical study of the transient solidification of a warm liquid flowing over a chilled flat plate. NASA Technical Note TN D-4015, Lewis Research Center, Cleveland, Ohio.

Schlichting, H. (1955) *Boundary Layer Theory*. New York: Pergamon Press.

Sieder, E.N. and G.E. Tate (1936) Heat transfer and pressure drop of liquids in tubes. *Industrial and Engineering Chemistry*, **28**: 1429–2435.

Stanley, L.E. (1967) A comparison of six thermistor calibration equations for exactness of fit to data from two configurations of bead thermistors—Pt. 1. USA Cold Regions Research and Engineering Laboratory, Technical Note (unpublished).

Vanoni, V.A. (1941) Velocity distribution in open channels. *Civil Engineering* **11**.

Vanoni, V.A. (1977) *ASCE Sedimentation Engineering*. American Society of Civil Engineers.

Von Karman, T. (1939) The analogy between fluid friction and heat transfer. *Transactions, American Society of Mechanical Engineers*, **61**: 705–710.

Yalin, A.M.S. (1977) *Mechanics of Sediment Transport*. New York: Pergamon Press.

Zisson, J.R. (1984) Experimental determination of heat transfer coefficients in water flowing over a horizontal ice sheet. M.E. Thesis, Thayer School of Engineering, Dartmouth College.

APPENDIX A: DATA ACQUISITION PROGRAM

```
10 DISP "FLUME DATA COLLECTION"
20 !
30 CLEAR 7
40 DISP
50 DISP "SET TIME BY TYPING SETTIME (HOUR OF DAY *3600 +MIN OF HOUR *6
0,(DAY OF MONTH)"
60 DISP "EX. SETTIME 8*3600+5*60,12"
70 DISP "PRESS CONT"
80 PAUSE
90 !
200 OPTION BASE 1
210 IMAGE 4D.DD
220 IMAGE 5D.DDD
230 DIM R(8),P(40),S(20,3),A(7),P1(50),P2(50),P3(50),P4(50),P5(50)
235 DIM L1(4),L2(4),T6(4),N1(4),N2(4),N4(4),N5(4),R5(4),R6(4),T(4)
240 MAT READ S
250 ! *************************
260 DEF FNV(T) = (-(.000004375*T^3)+.0013*T^2-.1488*T+7.9)*.00041339 !
 VISCOSITY OF WATER
270 DEF FNK(T) = (-(.00000111*T^2)+.0006889*T+.306)*1.7303 ! COND. OF
WATER
280 DEF FNP(T) = -(.00001563*T^3)+.004625*T^2-.5178*T+25.6 ! Pr no
290 DEF FND(T) = (62.23613+.012027*T-.00022038*T^2+.0000007951*T^3)*16
.018 ! DEN OF WATER>4
300 DEF FND1(T) = (.99987+.000006749996*T-.00000541659*T^2-.0000025000
35*T^3+4.1667167E-7*T^4)*1000
310 DEF FND2(T) = 1004.912359*(1.088-.001*T) ! DEN OF GYLCOL
320 DEF FNC2(T) = 1000*(2.961+.005*T) ! Cp OF GYLCOL
330 ! *************************
340 DISP "WHAT TYPE OF TEST IS THIS?"
350 DISP "TEMP/VEL PROFILE=1 "
360 DISP "ICE PROFILE=2"
390 DISP "MONITOR SYSTEM =5"
400 DISP "MONITOR ANY THERMISTER CHANNEL =6"
405 DISP "EXIT=7"
410 INPUT Z
420 PRINTER IS 2
430 !
435 K=0
450 IF Z=5 THEN 750
460 IF Z=6 THEN 4180
465 IF Z=7 THEN STOP
468 OUTPUT 707 ;""
469 PRINTER IS 707,80
470 ! *************************
471 ! LOAD 8300 PROGRAM
472 GOSUB 6700
473 WAIT 1000
474 CONTROL 10,9 ; 137
```

```
475 WAIT 1000
480 ! ENTER TEST IDENTIFICATION DATA
490 !
500 DISP "ENTER TEST NO. (____)" @ INPUT T$
510 CREATE T$,20
520 ASSIGN# 1 TO T$
530 DISP "ENTER DATE (__ MON 85)"
540 INPUT D$
550 DISP "ENTER WATER DEPTHS ,cm"
560 DISP "STATION 1 " @ INPUT D1(1)
570 DISP "STATION 2 " @ INPUT D1(2)
580 DISP "STATION 3 " @ INPUT D1(3)
590 DISP "STATION 4 " @ INPUT D1(4)
600 ! ENTRANCE LENGTHS ,METERS
610 L5(1)=10.55
620 L5(2)=10.86
630 L5(3)=11.164
640 L5(4)=11.465
650 DISP "ENTER FLOW RATES ,gal/min"
660 DISP "WATER" @ INPUT F1
670 DISP "COLD GLYCOL" @ INPUT F2
680 DISP "HOT GYLCOL" @ INPUT F3
690 DISP "HOT WATER" @ INPUT F4
700 !
710 ! SETS UP CALIBRATION CONSTANTS FOR HOT FILM
711 ! SENSOR #05
712 DISP "DATA IN PROGRAM IS FOR SENSOR #05"
713 DISP "INPUT RESISTANCE FOUND FROM WATER TEMP" @ INPUT T8
714 T8=-546.453+T8*98.002 ! Tef DEG C
715 DISP "INPUT THE RESISTANCE SETTING" @ INPUT R9@ R8=R9+.26+40
716 T9=-546.453+R9*98.002 ! Tsf DEG C
717 F9=T9*1.8+32
718 P9=6.48/R9*(R8/46.74)^2*((T9-T8)/61.74)*(FNK(F9)/FNK(191.48))
719 F7=(T9+T8)/2*1.8+32
720 Q9=P9*(FNV(135.91)/FND(135.91)/(FNV(F7)/FND(F7)))^.4*152.09033
721 P9=P9*36.4665
722 DISP "P9=";P9,"Q9=";Q9
723 DISP "VISCOSITY";FNV(F7)
730 ! ************************
740 !
750 ! NO ICE TEST OR MONITOR
760 !          SYSTEM
770 !
840 L1(1)=2.75121
850 L1(2)=4.7049
860 L1(3)=6.6572
870 L1(4)=8.6129
875 L2(1)=.012827
876 L2(2)=.01262
877 L2(3)=.0127
```

```
878 L2(4)=.01267
880 !
890 ! READ SYSTEM DATA CHANNELS
900 !
910 !
920 T=TIME/3600 ! TIME IN HRS
930 OUTPUT 709 ;"OPN"
940 OUTPUT 709 ;"CLS00"
960 OUTPUT 709 ;"F3N5RA0R5LSZ-8;T3"
970 ENTER 709 ; A(1),A(2),A(3),A(4),A(5),A(6),A(7)
980 OUTPUT 709 ;"OPN"
990 IF Z=2 THEN 2120
1000 !
1001 FOR I=1 TO 4
1002 H=19+I
1003 C=23+I
1004 R1=2*I
1005 R2=R1+1
1010 ! TAKE DATA AT EACH STATION
1020 !
1030 !
1040 OUTPUT 709 ;"OPN"
1050 OUTPUT 709 ;"DCV";H
1060 ENTER 709 ; H(I)
1070 OUTPUT 709 ;"TEM";C
1080 ENTER 709 ; T(I)
1090 OUTPUT 709 ;"OPN"
1100 IF I>1 THEN 1170
1110 OUTPUT 709 ;"OPN"
1120 OUTPUT 709 ;"CLS01"
1130 OUTPUT 709 ;"LSZ-9"
1140 OUTPUT 709 ;"F3N5RA0R5T3"
1150 ENTER 709 ; R(1),R(2),R(3),R(4),R(5),R(6),R(7),R(8)
1160 OUTPUT 709 ;"OPN"
1170 IF Z<>5 THEN GOSUB 2560 ! SUBROUTINE TO MOVE CARRIAGE
1180 !
1190 !
1200 !
1210 !
1220 !
1230 ! PROBE TEMPERATURES
1240 IF Z=5 THEN GOSUB 2750 @ GOTO 1640 ! SKIPS PROBE PROFILE
1260 IF I>1 THEN 1510
1430 CONTROL 10,9 ; 136
1440 DISP "NUMBER OF POINTS (Y POSITIONS)"
1450 INPUT I3
1460 DISP "INCREMENT, + IS UPWARD"
1470 INPUT I4
1480 DISP "# OF X-POSITIONS"
1490 INPUT I5
```

```
1500 REDIM P1(I3),P2(I3),P3(I3),P4(I3),P5(I3)
1510 FOR K=1 TO I5
1520 DISP "X-POSITION"
1530 INPUT X
1550 OUTPUT 10 "RUN 200"
1560 WAIT 500
1570 CONTROL 10,9 ; 141
1580 WAIT 1000
1590 OUTPUT 10 USING "K,K,K,K,K" ; X;",";I4;",";I3
1600 WAIT 1000
1610 CONTROL 10,9 ; 141
1620 GOSUB 1750
1630 NEXT K
1640 NEXT I
1650 IF Z=1 THEN GOSUB 6210
1655 IF Z=1 THEN ASSIGN# 1 TO *
1660 GOTO 340
1740 ! ************************
1745 ! SUBROUTINE FOR PROBE MEASUREMENTS
1750 FOR J=1 TO I3
1760 WAIT 6000
1770 P1(J)=I
1775 DISP "NOW READING X-Y COORD"
1780 ENTER 10 USING "#,K" ; P2(J)@ ENTER 10 USING "#,K" ; P3(J)
1785 P3(J)=-(1*P3(J))+.1
1786 P5(J)=0
1790 FOR K9=1 TO 10
1800 OUTPUT 703 ;"F1R-2RAZ1NST3"
1820 ENTER 703 ; P6 ! VELOCITY
1821 P5(J)=P5(J)+P6
1822 NEXT K9
1823 P5(J)=P5(J)/10
1827 OUTPUT 723 ;"F1R-2RAZ1NST3"
1828 ENTER 723 ; P4(J)
1840 CONTROL 10,9 ; 141
1850 OUTPUT 10 ;"CONT" @ WAIT 1000
1860 NEXT J
1870 GOSUB 2750
1880 RETURN
2110 ! ************************
2120 ! SUBPROGRAM TO PROFILE ICE
2130 DISP "ICE PROFILE SUBROUTINE"
2140 DISP "INPUT NUMBER OF READINGS"
2150 DISP "DETAILED = 150"
2160 DISP "GROSS    =  30"
2170 DISP "TEST     =   5" @ INPUT J9
2230 OUTPUT 709 ;"CLS01"
2240 OUTPUT 709 ;"LS2-9"
2250 OUTPUT 709 ;"F3N5RA0R5T3"
2270 ENTER 709 ; R(1),R(2),R(3),R(4),R(5),R(6),R(7),R(8)
```

```
2275 OUTPUT 709 ;"OPN"
2280 OUTPUT 709 ;"DCV20-23"
2290 ENTER 709 ; H(1),H(2),H(3),H(4)
2300 OUTPUT 709 ;"TEM24-27"
2320 ENTER 709 ; T(1),T(2),T(3),T(4)
2325 OUTPUT 709 ;"OPN"
2330 BEEP
2340 DISP "CARRIAGE SHOULD BE AT POINT 1 NOW"
2345 DISP "TURN ON CARRIAGE NOW"
2350 DISP "PRESS CONT WHEN READY" @ PAUSE
2360 FOR I=1 TO J9
2370 OUTPUT 709 ;"DCV28,29"
2380 ENTER 709 ; P1(I),P2(I) ! P1=CARRAGE,P2=ICE DEPTH
2390 BEEP
2400 WAIT 100
2405 NEXT I
2410 DISP "PAUSED" @ PAUSE
2420 ! CONVERT TEMP DATA
2430 FOR I=1 TO 4
2440 GOSUB 2750
2450 NEXT I
2460 ! CONVERT PROFILE DATA
2470 FOR I=1 TO J9
2480 P1(I)=P1(I)*15.54467 ! cm
2490 P2(I)=P2(I)*(10/(3*2.54)) ! cm
2500 PRINT I,P1(I),P2(I)
2510 NEXT I
2520 GOSUB 6220
2530 GOTO 340
2550 ! *************************
2560 ! SUB PROGRAM TO MOVE CARRIAGE
2590 DISP "MOVE CARRIAGE TO STATION ";I @ BEEP @ WAIT 100 @ BEEP
2600 DISP "ONE BEEP AND CARRAIGE IS IN CORRECT PLACE"
2610 DISP L1(I)
2620 WAIT 8000
2630 OUTPUT 709 ;"DCV28"
2640 ENTER 709 ; L
2650 DISP L
2660 IF L<L1(I)+.05 AND L>L1(I)-.05 THEN 2680 ELSE 2670
2670 BEEP @ WAIT 100 @ BEEP @ WAIT 100 @ BEEP @ GOTO 2620
2680 BEEP 150,300 @ DISP "AT POSITION ";I @ OUTPUT 709 ;"OPN" @ RETURN
2720 ! ***********************
2750 ! SUBPROGRAM TO CONVERT DATA
2760 DISP "CONVERTING DATA"
2770 ! CONVERTS DATA AND WRITES TO BUFFER
2775 IF K>1 THEN 3800
2780 IF I>1 THEN 3050
2790 FOR J1=1 TO 5
2800 A(J1)=1/(S(J1,1)+S(J1,2)*LOG(A(J1))+S(J1,3)*LOG(A(J1))^3)-273.15
2820 NEXT J1
```

```
2830 A(6)=1/(S(16,1)+S(16,2)*LOG(A(6))+S(16,3)*LOG(A(6))^3)-273.15
2840 A(7)=1/(S(17,1)+S(17,2)*LOG(A(7))+S(17,3)*LOG(A(7))^3)-273.15
2860 PRINT "TIME";T
2870 PRINT "AIR TEMP";
2880 PRINT USING 210 ; A(5)
2890 PRINT "FLUME ENTRANCE TEMP";
2900 PRINT USING 210 ; A(1)
2910 PRINT "FLUME EXIT TEMP";
2920 PRINT USING 210 ; A(2)
2930 PRINT "COLD GLYCOL ENTR";
2940 PRINT USING 210 ; A(4)
2950 PRINT "COLD GLYCOL EXIT";
2960 PRINT USING 210 ; A(3)
2970 PRINT "HOT GLYCOL ENTR";
2980 PRINT USING 210 ; A(6)
2990 PRINT "HOT GLYCOL EXIT";
3000 PRINT USING 210 ; A(7)
3010 PRINT
3020 IF Z<>5 THEN PRINT# 1 ; A(1),A(2),A(3),A(4),A(5),A(6),A(7),I3
3030 !
3040 I1=7 @ I2=8
3050 R(R1-1)=1/(S(I1,1)+S(I1,2)*LOG(R(R1-1))+S(I1,3)*LOG(R(R1-1))^3)-273.15
3060 R(R2-1)=1/(S(I2,1)+S(I2,2)*LOG(R(R2-1))+S(I2,3)*LOG(R(R2-1))^3)-273.15
3070 H(I)=H(I)*50000000*(-(.0014*(T(I)*1.8+32))+1.1)
3080 H(I)=H(I)/3.152 ! (W/m^2)
3090 K1=138 ! W/mC
3100 H1(I)=K1*(R(R2-1)-R(R1-1))/L2(I) ! W/m^2
3210 T6(I)=(R(R1-1)-R(R2-1))*(1.9144-1.5893)/(1.5893-.31864)+R(R1-1)
3220 IF Z=5 THEN GOTO 3510
3230 IF I>1 THEN GOTO 3510
3240 ! ENERGY ANALYSIS
3250 ! HEAD BOX TO TAIL BOX
3260 T1=A(2)-A(1)
3270 IF A(1)>4 THEN P1=FND((A(1)+A(2))/2*1.8+32)
3280 IF A(1)<=4 THEN P1=FND1((A(1)+A(2))/2)
3290 S1=4186 ! Cp OF WATER
3300 F1=F1*.0000630902 ! FLOW RATE IN m^3/SEC
3310 E1=S1*P1*T1*F1*.001 ! KWATTS
3320 ! COLD GLYCOL ENERGY
3330 T2=A(3)-A(4)
3340 S2=FNC2((A(4)+A(3))/2)
3350 P2=FND2((A(4)+A(3))/2)
3360 F2=F2*.0000630902
3370 E2=S2*P2*T2*F2*.001
3380 ! HOT GLYCOL ENERGY
3390 T3=A(6)-A(7)
3400 S3=FNC2((A(6)+A(7))/2)
3410 P3=FND2((A(6)+A(7))/2)
3420 F3=F3*.0000630902
3430 E3=S3*P3*T3*F3*.001
```

```
3440 IMAGE 4D.DDD
3450 PRINT "FLUME ENERGY ";
3460 PRINT USING 3440 ; E1
3470 PRINT "COLD GYLCOL EN";
3480 PRINT USING 3440 ; E2
3490 PRINT "HOT GYLCOL EN";
3500 PRINT USING 3440 ; E3
3510 IF Z<>5 THEN PRINT# 1 ; R(R1-1),R(R2-1),H(I),T(I)
3520 I1=I1+2 @ I2=I2+2
3530 !
3540 !
3550 PRINT
3551 IF Z=1 AND I=1 THEN OUTPUT 707
3552 IF Z=1 AND I=3 THEN OUTPUT 707
3555 IF Z=1 THEN GOTO 3760
3560 PRINT "STATION ";I
3570 PRINT "HEAT FLOW METER";
3580 PRINT USING 220 ; H(I)
3590 PRINT "HEAT FLOW X PLATE (.55)";
3600 PRINT USING 220 ; H1(I)
3630 PRINT "TEMP AT BOTTOM OF PLATE";T(I)
3640 PRINT "THERMISTER AT BOTTOM";
3650 PRINT USING 210 ; R(R2-1)
3660 PRINT "THERMISTER AT TOP ";
3670 PRINT USING 210 ; R(R1-1)
3680 IMAGE 3D.3D
3730 PRINT "CALC PLATE SURF";
3740 PRINT USING 210 ; T6(I)
3750 PRINT
3760 IF Z=5 THEN 4140
3770 IF Z=2 THEN 4140
3780 PRINT
3785 PRINT# 1 ; I3
3800 FOR J2=1 TO I3
3805 PRINT# 1 ; P5(J2)
3810 P4(J2)=.13573+25.44371*(P4(J2)*1000)
3815 P5(J2)=((P5(J2)^2-P9)/Q9)^2.5*.3048
3820 NEXT J2
3821 PRINTER IS 707,80
3822 OUTPUT 707 ;""
3823 IMAGE 5X,"STATION",6X,"XCOORD",5X,"YCOORD",4X,"TEMP(C)",4X,"VEL(M/S)"
3824 PRINT USING 3823
3829 IMAGE 7X,D,10X,2D.2D,6X,2D.2D,5X,2D.2D,7X,2D.2D
3830 FOR M=1 TO I3
3831 IMAGE 7X,D,10X,2D.2D,6X,2D.2D,5X,2D.2D,7X,2D.2D
3832 PRINT USING 3829 ; P1(M),P2(M),P3(M),P4(M),P5(M)
3835 PRINT# 1 ; P1(M),P2(M),P3(M),P4(M),P5(M)
3837 NEXT M
3838 PRINT @ PRINT @ PRINT
3839 IF K>1 THEN 4140
```

```
3840 ! CALCULATE Re AND Nu
3850 !
3860 B1=P4(3)*1.8+32 ! BULK TEMP
3870 B2=T6(I)*1.8+32 ! SURFACE TEMP
3880 B3=(B1+B2)/2 ! FILM TEMP
3890 B9=(B3-32)/1.8
3900 IF B9<=4 THEN B4=FND1(B9) ! DEN WATER <= 4
3910 IF B9>4 THEN B4=FND(B3) ! DEN WATER >4
3920 B8=FNV(B3)/B4 ! DYNAMIC VISCSITY
3930 B5=FNK(B3)
3940 B7=FNP(B3) ! PRANDTL NO
3950 H1=H(I)/(T6(I)-P4(3))
3960 H2=H1(I)/(T6(I)-P4(3))
3980 V1(I)=F1/(30.48*D1(I)/(100*100))
3990 H9=4*30.48*D1(I)/(2*D1(I)+30.48)/100
4000 R5(I)=V1(I)*H9/B8 ! Re,Hd
4010 R6(I)=V1(I)*L5(I)/B8 ! Re,L
4020 N1(I)=H1*H9/B5 ! Nu,Hd
4030 N2(I)=H2*H9/B5
4050 N4(I)=H1*L5(I)/B5
4060 N5(I)=H2*L5(I)/B5
4080 PRINT "K OF WATER";B5
4090 PRINT "HEAT TRAN CO";H2
4100 PRINT "HYDR DIAM";H9
4110 PRINT "VISCOSITY OF WATER";B8
4120 PRINT "VELOCITY OF WATER";V1(I)
4130 PRINT "DENSITY OF WATER ";B4
4140 RETURN
4150 !
4160 !
4170 !
4180 ! MONITORS ANY THERMISTER  CHANNEL
4190 CLEAR 709
4200 DISP "WHICH CHANNEL?" @ INPUT G
4210 DISP "NUMBER OF READINGS?" @ INPUT G1
4220 DISP "TIME BETWEEN READINGS (SEC)?" @ INPUT G2@ G2=G2*1000
4230 IF G<>1 THEN GOTO 4340
4240 FOR I=1 TO G1
4250 OUTPUT 709 ;"CLS0"
4260 OUTPUT 709 ;"F3N5RA0R5LS2;T3"
4270 ENTER 709 ; G3
4280 G4=1/(S(1,1)+S(1,2)*LOG(G3)+S(1,3)*LOG(G3)^3)-273.15
4290 OUTPUT 709 ;"OPN"
4300 PRINT USING 210 ; G4
4310 WAIT G2
4320 NEXT I
4330 GOTO 350
4340 IF G<>2 THEN GOTO 4450
4350 FOR I=1 TO G1
4360 OUTPUT 709 ;"CLS0"
```

```
4370 OUTPUT 709 ;"F3N5RA0R5LS3;T3"
4380 ENTER 709 ; G3
4390 OUTPUT 709 ;"OPN"
4400 G4=1/(S(2,1)+S(2,2)*LOG(G3)+S(2,3)*LOG(G3)^3)-273.15
4410 PRINT USING 210 ; G4
4420 WAIT G2
4430 NEXT I
4440 GOTO 350
4450 IF G<>3 THEN GOTO 4550
4460 FOR I=1 TO G1
4470 OUTPUT 709 ;"CLS0"
4480 OUTPUT 709 ;"F3N5RA0R5LS4;T3"
4490 ENTER 709 ; G3
4500 OUTPUT 901 ;"OPN"
4510 G4=1/(S(3,1)+S(3,2)*LOG(G3)+S(3,3)*LOG(G3)^3)-273.15
4520 PRINT USING 210 ; G4
4530 WAIT G2 @ NEXT I
4540 GOTO 350
4550 IF G<>4 THEN GOTO 4660
4560 FOR I=1 TO G1
4570 OUTPUT 709 ;"CLS0"
4580 OUTPUT 709 ;"LS5"
4590 OUTPUT 709 ;"F3N5RA0R5LS5;T3"
4600 ENTER 709 ; G3
4610 OUTPUT 709 ;"OPN"
4620 G4=1/(S(4,1)+S(4,2)*LOG(G3)+S(4,3)*LOG(G3)^3)-273.15
4630 PRINT USING 210 ; G4
4640 WAIT G2 @ NEXT I
4650 GOTO 350
4660 IF G<>5 THEN GOTO 4770
4670 FOR I=1 TO G1
4680 OUTPUT 709 ;"CLS0"
4690 OUTPUT 709 ;"LS6"
4700 OUTPUT 709 ;"F3N5RA0R5T3"
4710 ENTER 709 ; G3
4720 OUTPUT 709 ;"OPN"
4730 G4=1/(S(5,1)+S(5,2)*LOG(G3)+S(5,3)*LOG(G3)^3)-273.15
4740 PRINT USING 210 ; G4
4750 WAIT G2 @ NEXT I
4760 GOTO 350
4770 IF G<>6 THEN GOTO 4880
4780 FOR I=1 TO G1
4790 OUTPUT 709 ;"CLS0"
4800 OUTPUT 709 ;"LS7"
4810 OUTPUT 709 ;"F3N5RA0R5T3"
4820 ENTER 709 ; G3
4830 OUTPUT 709 ;"OPN"
4840 G4=1/(S(16,1)+S(16,2)*LOG(G3)+S(16,3)*LOG(G3)^3)-273.15
4850 PRINT USING 210 ; G4
4860 WAIT G2 @ NEXT I
```

```
4870 GOTO 350
4880 IF G<>7 THEN GOTO 4990
4890 FOR I=1 TO G1
4900 OUTPUT 709 ;"CLS0"
4910 OUTPUT 709 ;"LS8"
4920 OUTPUT 709 ;"F3N5RA0R5T3"
4930 ENTER 709 ; G3
4940 OUTPUT 709 ;"OPN"
4950 G4=1/(S(17,1)+S(17,2)*LOG(G3)+S(17,3)*LOG(G3)^3)-273.15
4960 PRINT USING 210 ; G4
4970 WAIT G2 @ NEXT I
4980 GOTO 350
4990 IF G<>8 THEN GOTO 5100
5000 FOR I=1 TO G1
5010 OUTPUT 709 ;"CLS0"
5020 OUTPUT 709 ;"LS9"
5030 OUTPUT 709 ;"F3N5RA0R5T3"
5040 ENTER 709 ; G3
5050 OUTPUT 709 ;"OPN"
5060 G4=1/(S(6,1)+S(6,2)*LOG(G3)+S(6,3)*LOG(G3)^3)-273.15
5070 PRINT USING 210 ; G4
5080 WAIT G2 @ NEXT I
5090 GOTO 350
5100 IF G<>9 THEN GOTO 5210
5110 FOR I=1 TO G1
5120 OUTPUT 709 ;"CLS1"
5130 OUTPUT 709 ;"LS2"
5140 OUTPUT 709 ;"F3N5RA0R5T3"
5150 ENTER 709 ; G3
5160 OUTPUT 709 ;"OPN"
5170 G4=1/(S(7,1)+S(7,2)*LOG(G3)+S(7,3)*LOG(G3)^3)-273.15
5180 PRINT USING 210 ; G4
5190 WAIT G2 @ NEXT I
5200 GOTO 350
5210 IF G<>10 THEN GOTO 5320
5220 FOR I=1 TO G1
5230 OUTPUT 709 ;"CLS1"
5240 OUTPUT 709 ;"LS3"
5250 OUTPUT 709 ;"F3N5RA0R5T3"
5260 ENTER 709 ; G3
5270 OUTPUT 709 ;"OPN"
5280 G4=1/(S(8,1)+S(8,2)*LOG(G3)+S(8,3)*LOG(G3)^3)-273.15
5290 PRINT USING 210 ; G4
5300 WAIT G2 @ NEXT I
5310 GOTO 350
5320 IF G<>11 THEN GOTO 5440
5330 OUTPUT 709 ;"CLS1"
5340 FOR I=1 TO G1
5350 OUTPUT 709 ;"CLS1"
5360 OUTPUT 709 ;"LS4"
```

```
5370 OUTPUT 709 ;"F3N5RA0R5T3"
5380 ENTER 709 ; G3
5390 OUTPUT 709 ;"OPN"
5400 G4=1/(S(9,1)+S(9,2)*LOG(G3)+S(9,3)*LOG(G3)^3)-273.15
5410 PRINT USING 210 ; G4
5420 WAIT G2 @ NEXT I
5430 GOTO 350
5440 IF G<>12 THEN GOTO 5550
5450 FOR I=1 TO G1
5460 OUTPUT 709 ;"CLS1"
5470 OUTPUT 709 ;"LS5"
5480 OUTPUT 709 ;"F3N5RA0R5T3"
5490 ENTER 709 ; G3
5500 OUTPUT 709 ;"OPN"
5510 G4=1/(S(10,1)+S(10,2)*LOG(G3)+S(10,3)*LOG(G3)^3)-273.15
5520 PRINT USING 210 ; G4
5530 WAIT G2 @ NEXT I
5540 GOTO 350
5550 IF G<>13 THEN GOTO 5660
5560 FOR I=1 TO G1
5570 OUTPUT 709 ;"CLS1"
5580 OUTPUT 709 ;"LS6"
5590 OUTPUT 709 ;"F3N5RA0R5T3"
5600 ENTER 709 ; G3
5610 OUTPUT 709 ;"OPN"
5620 G4=1/(S(11,1)+S(11,2)*LOG(G3)+S(11,3)*LOG(G3)^3)-273.15
5630 PRINT USING 210 ; G4
5640 WAIT G2 @ NEXT I
5650 GOTO 350
5660 IF G<>14 THEN GOTO 5770
5670 FOR I=1 TO G1
5680 OUTPUT 709 ;"CLS1"
5690 OUTPUT 709 ;"LS7"
5700 OUTPUT 709 ;"F3N5RA0R5T3"
5710 ENTER 709 ; G3
5720 OUTPUT 709 ;"OPN"
5730 G4=1/(S(12,1)+S(12,2)*LOG(G3)+S(12,3)*LOG(G3)^3)-273.15
5740 PRINT USING 210 ; G4
5750 WAIT G2 @ NEXT I
5760 GOTO 350
5770 IF G<>15 THEN GOTO 5870
5780 FOR I=1 TO G1
5790 OUTPUT 709 ;"CLS1"
5800 OUTPUT 709 ;"LS8"
5810 OUTPUT 709 ;"F3N5RA0R5T3"
5820 ENTER 709 ; G3
5830 OUTPUT 709 ;"OPN"
5840 G4=1/(S(13,1)+S(13,2)*LOG(G3)+S(13,3)*LOG(G3)^3)-273.15
5850 PRINT USING 210 ; G4
5860 WAIT G2 @ NEXT I
```

```
5870 IF G<>16 THEN GOTO 5970
5880 FOR I=1 TO G1
5890 OUTPUT 709 ;"CLS1"
5900 OUTPUT 709 ;"LS9"
5910 OUTPUT 709 ;"F3NSRA0RST3"
5920 ENTER 709 ; G3
5930 OUTPUT 709 ;"OPN"
5940 G4=1/(S(14,1)+S(14,2)*LOG(G3)+S(14,3)*LOG(G3)^3)-273.15
5950 PRINT USING 210 ; G4
5960 WAIT G2 @ NEXT I
5970 DISP "NOSUCH CHANNEL"
5980 GOTO 350
5990 !
6000 ! ***********************
6010 DATA .0013217799,.00025777108,1.7435609E-7
6020 DATA .0013546937,.0002530644,1.8275039E-7
6030 DATA .0013105286,.00025873507,1.7603274E-7
6040 DATA .001348592,.00025330525,1.5758163E-7
6050 DATA .001302763,.00026117401,1.6079275E-7
6060 DATA .0013181985,.00026139129,1.3640022E-7
6070 DATA .0013343537,.00025692141,1.6000615E-7
6080 DATA .0013037492,.00025949184,1.666341E-7
6090 DATA .0013348872,.00025676909,1.6407671E-7
6100 DATA .0013526671,.00025602699,1.5699062E-7
6110 DATA .0013006584,.00025973931,1.6871901E-7
6120 DATA .0013503701,.00025502833,1.5168687E-7
6130 DATA .0013124103,.0002594037,1.7012861E-7
6140 DATA .0013027286,.00025987376,1.6883065E-7
6150 DATA .0013343537,.00025692141,1.6000615E-7
6160 DATA .0013545896,.00025492581,1.5161931E-7
6170 DATA .0013122181,.00025971489,1.628156E-7
6180 DATA .0013348872,.00025676909,1.6407671E-7
6190 DATA .001310042,.00025963523,1.6717593E-7
6200 DATA .0013217799,.00025777108,1.7435609E-7
6210 !
6220 PRINTER IS 707,80
6230 OUTPUT 707 ;""
6235 OUTPUT 707
6240 PRINT "Test no. ";T$
6250 Z=IP(T)
6260 Z1=IP((T-Z)*60) ! MIN
6270 IMAGE "TIME",1X,2D,":",2D
6280 PRINT USING 6270 ; Z,Z1
6290 PRINT D$
6300 IMAGE 3D," gal/min"
6310 PRINT "FLOW RATE:";@ PRINT USING 6300 ; F1/.0000630902
6320 IMAGE 3D.2D," Deg C"
6330 PRINT "BULK WATER TEMP";@ PRINT USING 6320 ; P4(3)
6340 PRINT "PRANDTL NO. ";
6350 PRINT USING 210 ; B7
```

```
6360 PRINT
6370 IMAGE 14X,"STATION 1",3X,"STATION 2",3X,"STATION 3",3X,"STATION 4"
6380 PRINT USING 6370
6390 PRINT
6400 PRINT "PLATE TEMP"
6410 PRINT " @ 0 cm   ";
6420 IMAGE 5X,3D.2D,6X,3D.2D,6X,3D.2D,6X,3D.2D
6430 PRINT USING 6420 ; T(1),T(2),T(3),T(4)
6440 PRINT " @ .325 cm";@ PRINT USING 6420 ; R(2),R(4),R(6),R(8)
6450 PRINT " @ 1.59 cm";@ PRINT USING 6420 ; R(1),R(3),R(5),R(7)
6455 PRINT "@ 1.914 cm";@ PRINT USING 6420 ; T6(1),T6(2),T6(3),T6(4)
6460 IMAGE 8X,6D.2D,5X,6D.2D,5X,6D.2D,5X,6D.2D
6470 PRINT
6480 PRINT "HEAT FLOW"
6490 PRINT "METER";@ PRINT USING 6460 ; H(1),H(2),H(3),H(4)
6500 PRINT "X .55";@ PRINT USING 6460 ; H1(1),H1(2),H1(3),H1(4)
6520 PRINT
6530 IMAGE 5X,7D,6X,7D,6X,7D,6X,7D
6540 PRINT "REYNOLDS NUMBER"
6550 PRINT " HYDR DIAM";@ PRINT USING 6530 ; R5(1),R5(2),R5(3),R5(4)
6560 PRINT " ENTR LEN ";@ PRINT USING 6530 ; R6(1),R6(2),R6(3),R6(4)
6570 IMAGE 11X,6D,8X,6D,8X,6D,8X,6D
6580 PRINT
6590 PRINT "NUSSELT NUMBER, HYDR. DIAM"
6600 PRINT "METER";@ PRINT USING 6570 ; N1(1),N1(2),N1(3),N1(4)
6610 PRINT "X .55";@ PRINT USING 6570 ; N2(1),N2(2),N2(3),N2(4)
6630 PRINT
6640 PRINT "NUSSELT NO., ENTR. LEN."
6650 PRINT " METER";@ PRINT USING 6570 ; N4(1),N4(2),N4(3),N4(4)
6660 PRINT " X .55";@ PRINT USING 6570 ; N5(1),N5(2),N5(3),N5(4)
6680 RETURN
6690 END
6700 ! EXTERNAL SUBROUTINE
6710 ! TO SET UP MOTOR CONTROL
6720 ! MOTOR CONTROL ADDRESS
6730 ! IS 10
6740 !
6750 DISP "SET PROBE TO (0,0)"
6760 DISP "PRESS CONT WHEN READY" @ PAUSE
6770 ! SETUP HP-IL/RS232C INTERFACE
6780 CONTROL 10,3 ; 6
6790 CONTROL 10,4 ; 10
6800 CONTROL 10,12 ; 94
6810 CONTROL 10,13 ; 13
6820 CONTROL 10,14 ; 63
6830 CONTROL 10,16 ; 1
6840 CONTROL 10,17 ; 13
6850 CONTROL 10,9 ; 136
```

```
6860 ! UNITS WILL BE CENTIMETERS
6870 DISP "6650"
6880 OUTPUT 10 ;"E"
6890 DISP "6670"
6900 WAIT 2000
6920 !
6930 OUTPUT 10 ;"0 I2=-I2:IFA2<>P2 THEN A2=-A2"
6940 WAIT 2000
7190 OUTPUT 10 ;"200 P=1:INPUT X,S6,S7"
7200 OUTPUT 10 ;"205 GOSUB 1000:A1=X:@:A2=0:@"
7220 DISP "6970"
7230 OUTPUT 10 ;"210 GOSUB 500:STOP:FOR Q=1 TO (S7-1)"
7240 WAIT 1000
7250 ! OUTPUT 10 ;"220 IF(P1-.5)<-19.8 THEN240"
7260 DISP "7010"
7280 OUTPUT 10 ;"230 I2=S6:@:GOSUB 500:STOP:NEXT Q"
7300 OUTPUT 10 ;"240 A1=0:@:A2=0:@:END"
7310 DISP "7060"
7595 OUTPUT 10 ;"500 P6=INT(P1*10^2+.5)/10^2:P7=INT(P2*10^2+.5)/10^2"
7596 WAIT 2000
7600 OUTPUT 10 ;"510 PRINT P6:PRINT P7:RETURN"
7620 DISP "7370"
7630 OUTPUT 10 ;"1000 C1=.000635:C2=.000635:R1=1:R2=R1"
7650 DISP "7400"
7660 OUTPUT 10 ;"1010 V1=900:V2=V1:D1=10:RETURN"
7670 DISP "7420"
7680 RETURN
7690 END
```

APPENDIX B: TYPICAL DATA OUTPUT, TEST 066

Test no. 0066
TIME 13:47
6 AUG 86
FLOW RATE:400 gal/min
BULK WATER TEMP 8.28 Deg C
PRANDTL NO. 10.11

	STATION 1	STATION 2	STATION 3	STATION 4
PLATE TEMP				
@ 0 cm	3.73	4.93	4.00	5.11
@ .325 cm	6.19	6.62	6.47	6.59
@ 1.59 cm	6.53	6.87	6.77	6.86
@ 1.914 cm	6.62	6.93	6.84	6.93
HEAT FLOW				
METER	-364.97	-198.50	-248.68	-181.88
X .55	-3634.36	-2657.30	-3210.97	-2928.59
REYNOLDS NUMBER				
HYDR DIAM	116411	116890	116760	116830
ENTR LEN	3995518	4129839	4240749	4357679
NUSSELT NUMBER, HYDR. DIAM				
METER	111	76	89	72
X .55	1109	1016	1150	1155
NUSSELT NO., ENTR. LEN.				
METER	3821	2682	3236	2676
X .55	38053	35898	41784	43094

TIME 13.7897958333
AIR TEMP 25.73
FLUME ENTRANCE TEMP 8.68
FLUME EXIT TEMP 8.59
COLD GLYCOL ENTR -27.11
COLD GLYCOL EXIT -25.47
HOT GLYCOL ENTR 11.54
HOT GLYCOL EXIT 11.25

FLUME ENERGY -9.265
COLD GYLCOL EN 11.472
HOT GYLCOL EN 0.000

STATION	XCOORD	YCOORD	TEMP(C)	VEL(M/S)
1	0.00	.10	8.19	.02
1	0.00	1.10	8.33	.02
i	0.00	2.10	8.35	.02
1	0.00	3.10	8.42	.02
1	0.00	4.10	8.40	.02
1	0.00	5.10	8.42	.02
1	0.00	6.10	8.43	.02
1	0.00	7.10	8.45	.02
1	0.00	8.10	8.46	.02
1	0.00	9.10	8.47	.02
1	0.00	10.10	8.48	.02
1	0.00	11.10	8.48	.02
1	0.00	12.10	8.49	.02
1	0.00	13.10	8.50	.02

K OF WATER .579704283168
HEAT TRAN CO 2090.96338324
HYDR DIAM .307378009109
VISCOSITY OF WATER 1.41044008718E-6
VELOCITY OF WATER .534164761663
DENSITY OF WATER 999.556769831

STATION	XCOORD	YCOORD	TEMP(C)	VEL(M/S)
2	0.00	.10	8.17	.02
2	0.00	1.10	8.25	.02
2	0.00	2.10	8.31	.02
2	0.00	3.10	8.37	.02
2	0.00	4.10	8.39	.02
2	0.00	5.10	8.41	.02
2	0.00	6.10	8.40	.02
2	0.00	7.10	8.43	.02
2	0.00	8.10	8.44	.02
2	0.00	9.10	8.47	.02
2	0.00	10.10	8.47	.02
2	0.00	11.10	8.47	.02
2	0.00	12.10	8.48	.02
2	0.00	13.10	8.49	.02

K OF WATER .579951897005
HEAT TRAN CO 1917.05079022
HYDR DIAM .307378009109
VISCOSITY OF WATER 1.40466247544E-6
VELOCITY OF WATER .534164761663
DENSITY OF WATER 999.54463703

STATION	XCOORD	YCOORD	TEMP(C)	VEL(M/S)
3	0.00	.10	8.25	.02
3	0.00	1.10	8.25	.02
3	0.00	2.10	8.32	.02
3	0.00	3.10	8.34	.02
3	0.00	4.10	8.33	.02
3	0.00	5.10	8.37	.02
3	0.00	6.10	8.39	.02
3	0.00	7.10	8.41	.02
3	0.00	8.10	8.40	.02
3	0.00	9.10	8.42	.02
3	0.00	10.10	8.44	.02
3	0.00	11.10	8.45	.02
3	0.00	12.10	8.47	.02
3	0.00	13.10	8.44	.02

K OF WATER .579885136096
HEAT TRAN CO 2170.35066979
HYDR DIAM .307378009109
VISCOSITY OF WATER 1.40621733823E-6
VELOCITY OF WATER .534164761663
DENSITY OF WATER 999.547930213

STATION	XCOORD	YCOORD	TEMP(C)	VEL(M/S)
4	0.00	.10	8.19	.02
4	0.00	1.10	8.23	.02
4	0.00	2.10	8.28	.02
4	0.00	3.10	8.32	.02
4	0.00	4.10	8.35	.02
4	0.00	5.10	8.32	.02
4	0.00	6.10	8.37	.02
4	0.00	7.10	8.35	.02
4	0.00	8.10	8.38	.02
4	0.00	9.10	8.43	.02
4	0.00	10.10	8.40	.02
4	0.00	11.10	8.43	.02
4	0.00	12.10	8.43	.02
4	0.00	13.10	8.45	.02

K OF WATER .579921040138
HEAT TRAN CO 2179.75455364
HYDR DIAM .307378009109
VISCOSITY OF WATER 1.40538086839E-6
VELOCITY OF WATER .534164761663
DENSITY OF WATER 999.546161154

APPENDIX C: TEST DATA AND CALCULATED PARAMETERS

Notes:

(1) Lower thermistor in flume bed.
(2) Upper thermistor in flume bed.
(3) Calculated bed surface temperature.
(4) Reynolds number using velocity correction.
(5) Velocity correction is not applicable to low flow rates.
(6) Entries 116–119 were not included; these data were not at steady state.

Flume bed temperature above 4 degrees C, turbulent flow

Entry No.	Station No.	Temperature at (1) (degrees C)	Temperature at (2) (degrees C)	Temperature at (3) (degrees C)	Flow Rate (GPM)	Water Depth (cm)	Bulk Temp (C)	Pr no	Hydraulic Diameter Re	Hydraulic Diameter Re(4)	Hydraulic Diameter Nu	Entrance Length Re	Entrance Length Nu	Heat Flux (W/m^2)
1	2	6.50	6.83	6.92	170	14.5	10.7	9.1	56362	75989	489	1.95E+06	1.80E+04	3608.6
2	3	6.27	6.54	6.61	170	14.5	10.7	9.1	56394	75975	366	2.00E+06	1.38E+04	2933.9
3	4	6.34	6.67	6.75	170	14.5	10.6	9.1	56329	75909	470	2.05E+06	1.82E+04	3594.3
4	2	6.58	6.91	7.00	170	14.5	10.7	9.1	56394	76054	497	1.95E+06	1.83E+04	3608.6
5	3	6.35	6.64	6.71	170	14.5	10.7	9.1	56362	75948	405	2.00E+06	1.53E+04	3151.2
6	4	6.42	6.76	6.85	170	14.5	10.7	9.1	56378	75999	492	2.06E+06	1.91E+04	3703.2
7	2	6.33	6.65	6.73	170	14.0	10.5	9.2	57018	77051	466	2.01E+06	1.75E+04	3499.2
8	3	6.05	6.37	6.45	170	14.0	10.5	9.2	57010	76981	431	2.05E+06	1.66E+04	3477.2
9	4	6.06	6.40	6.49	170	14.0	10.4	9.2	56961	76915	467	2.11E+06	1.85E+04	3703.2
10	2	6.28	6.60	6.68	170	14.0	10.4	9.2	56927	76906	467	2.00E+06	1.75E+04	3499.2
11	3	6.00	6.32	6.40	170	14.0	10.4	9.2	56894	76800	434	2.05E+06	1.67E+04	3477.2
12	4	6.03	6.38	6.47	170	14.0	10.4	9.2	56861	76765	486	2.11E+06	1.92E+04	3812.2
13	2	7.08	7.41	7.50	220	13.5	10.5	9.2	75149	106649	586	2.73E+06	2.23E+04	3608.6
14	3	6.82	7.15	7.23	220	13.5	10.5	9.2	75149	106580	535	2.79E+06	2.10E+04	3585.8
15	4	6.91	7.27	7.36	220	13.5	10.5	9.2	75061	106479	617	2.87E+06	2.48E+04	3921.1
16	2	7.08	7.41	7.50	220	13.5	10.5	9.2	75171	106682	584	2.73E+06	2.22E+04	3608.6
17	3	6.84	7.16	7.24	220	13.5	10.5	9.2	75127	106548	522	2.79E+06	2.05E+04	3477.2
18	4	6.91	7.27	7.36	220	13.5	10.5	9.2	75105	106546	613	2.87E+06	2.47E+04	3921.1
19	2	4.28	4.55	4.62	100	14.5	10.5	9.2	32952	39922	257	1.10E+06	9.49E+03	2952.5
20	3	4.03	4.27	4.33	100	14.5	10.5	9.2	32981	39925	215	1.13E+06	8.17E+03	2607.9
21	4	3.93	4.22	4.29	100	14.5	10.5	9.2	33010	39959	258	1.16E+06	1.01E+04	3158.6
22	2	4.29	4.54	4.60	100	14.5	10.4	9.2	32943	39907	238	1.10E+06	8.78E+03	2733.8
23	3	4.02	4.27	4.33	100	14.5	10.4	9.2	32943	39874	226	1.13E+06	8.57E+03	2716.5
24	4	3.91	4.19	4.26	100	14.5	10.4	9.2	32876	39776	254	1.16E+06	9.88E+03	3049.7
25	2	4.36	4.59	4.65	100	14.5	10.5	9.2	32952	39925	220	1.10E+06	8.12E+03	2515.1
26	3	4.06	4.31	4.37	100	14.5	10.4	9.2	32933	39866	228	1.13E+06	8.64E+03	2716.5
27	4	3.95	4.22	4.29	100	14.5	10.4	9.2	32905	39818	244	1.16E+06	9.52E+03	2940.8
28	2	6.58	6.86	6.93	150	14.0	10.5	9.2	50318	66536	430	1.78E+06	1.61E+04	3061.8
29	3	6.35	6.61	6.68	150	14.0	10.5	9.2	50303	66469	371	1.82E+06	1.43E+04	2825.2
30	4	6.37	6.66	6.73	150	14.0	10.4	9.2	50245	66395	426	1.87E+06	1.68E+04	3158.6
31	2	6.55	6.84	6.91	150	14.0	10.4	9.2	50186	66343	455	1.77E+06	1.70E+04	3171.2
32	3	6.32	6.59	6.66	150	14.0	10.3	9.2	50113	66191	398	1.82E+06	1.53E+04	2933.9
33	4	6.33	6.64	6.72	150	14.0	10.3	9.2	50113	66202	465	1.87E+06	1.84E+04	3376.5
34	2	7.11	7.41	7.49	200	13.5	10.4	9.2	68139	95153	548	2.48E+06	2.09E+04	3280.5
35	3	6.89	7.19	7.27	200	13.5	10.4	9.2	68039	94949	514	2.53E+06	2.01E+04	3259.8
36	4	6.93	7.24	7.32	200	13.5	10.4	9.2	68099	95052	536	2.61E+06	2.16E+04	3376.5
37	2	7.12	7.41	7.48	200	13.5	10.4	9.2	68099	95092	532	2.47E+06	2.03E+04	3171.2
38	3	6.90	7.19	7.26	200	13.5	10.4	9.2	68039	94979	495	2.53E+06	1.94E+04	3151.2
39	4	6.95	7.26	7.34	200	13.5	10.4	9.2	68020	94937	547	2.60E+06	2.20E+04	3376.5
40	2	7.74	8.02	8.09	247	14.0	10.3	9.2	82520	119189	680	2.97E+06	2.54E+04	3061.8
41	3	7.48	7.85	7.94	247	13.9	10.3	9.2	82779	119573	837	3.07E+06	3.23E+04	4020.5
42	4	7.48	7.81	7.89	247	13.8	10.3	9.2	83016	119952	737	3.17E+06	2.93E+04	3594.3
43	2	7.78	8.06	8.13	247	14.0	10.3	9.2	82520	119201	692	2.97E+06	2.58E+04	3061.8
44	3	7.52	7.90	8.00	247	13.9	10.4	9.2	82827	119664	872	3.07E+06	3.36E+04	4129.1
45	4	7.52	7.86	7.95	247	13.8	10.3	9.2	83040	120005	773	3.17E+06	3.07E+04	3703.2
46	2	8.89	9.10	9.15	300	13.8	10.7	9.1	101918	152522	745	3.74E+06	2.80E+04	2296.4
47	3	8.75	9.00	9.06	300	13.7	10.7	9.1	102300	153124	823	3.86E+06	3.19E+04	2716.5

Entry No.	Station No.	Temperature at (1) (degrees C)	(2)	(3)	Flow Rate (GPM)	Water Depth (cm)	Bulk Temp (C)	Pr no	Hydraulic Diameter Re	Re(4)	Nu	Entrance Length Re	Nu	Heat Flux (W/m^2)
48	4	8.80	9.03	9.09	300	13.7	10.7	9.1	102270	153085	776	3.97E+06	3.09E+04	2505.1
49	2	8.96	9.17	9.22	300	13.8	10.6	9.1	101712	152213	820	3.74E+06	3.08E+04	2296.4
50	3	8.83	9.07	9.13	300	13.7	10.6	9.1	102152	152908	851	3.87E+06	3.30E+04	2607.9
51	4	8.87	9.10	9.16	300	13.7	10.6	9.1	102152	152918	833	3.97E+06	3.32E+04	2505.1
52	2	8.89	9.18	9.25	350	13.5	10.5	9.2	119520	183357	1246	4.45E+06	4.74E+04	3171.1
53	3	8.86	9.11	9.17	350	13.5	10.5	9.2	119520	183323	1001	4.57E+06	3.91E+04	2716.5
54	4	8.92	9.15	9.21	350	13.5	10.5	9.2	119485	183281	956	4.70E+06	3.84E+04	2505.1
55	2	9.01	9.22	9.27	350	13.5	10.5	9.2	119555	183422	909	4.45E+06	3.45E+04	2296.4
56	3	8.89	9.14	9.20	350	13.5	10.5	9.2	119520	183336	1025	4.57E+06	4.00E+04	2716.5
57	4	8.85	9.17	9.25	350	13.5	10.5	9.2	119520	183356	1365	4.70E+06	5.48E+04	3485.4
58	2	9.16	9.37	9.42	400	13.3	10.6	9.2	137751	215860	990	5.18E+06	3.79E+04	2296.4
59	3	9.05	9.31	9.38	400	13.3	10.6	9.2	137751	215837	1167	5.32E+06	4.59E+04	2825.2
60	4	9.10	9.33	9.39	400	13.3	10.6	9.1	137791	215911	1038	5.47E+06	4.20E+04	2505.1
61	2	9.22	9.44	9.50	400	13.3	10.5	9.2	137711	215827	1119	5.19E+06	4.29E+04	2405.7
62	3	9.12	9.37	9.43	400	13.3	10.6	9.2	137751	215864	1180	5.33E+06	4.64E+04	2716.5
63	4	9.17	9.40	9.46	400	13.2	10.6	9.1	138276	216766	1099	5.51E+06	4.46E+04	2505.1
64	2	9.28	9.49	9.54	450	13.0	10.4	9.2	155845	248651	1318	5.96E+06	5.11E+04	2296.4
65	3	9.19	9.45	9.52	450	13.0	10.4	9.2	155754	248481	1604	6.12E+06	6.39E+04	2825.2
66	4	9.24	9.47	9.53	450	12.9	10.4	9.2	156353	249513	1422	6.34E+06	5.84E+04	2505.1
67	2	9.27	9.48	9.53	450	13.0	10.3	9.2	155663	248336	1367	5.95E+06	5.30E+04	2296.3
68	3	9.18	9.43	9.49	450	13.0	10.4	9.2	155709	248391	1520	6.12E+06	6.05E+04	2716.5
69	4	9.23	9.45	9.51	450	12.9	10.4	9.2	156490	249735	1280	6.34E+06	5.26E+04	2396.2
232	1	5.50	5.77	5.83	200	31.4	13.4	8.4	45451	58308	268	1.05E+06	6.97E+03	2904.8
233	2	6.62	6.86	6.92	200	31.4	13.4	8.4	45451	58561	285	1.10E+06	7.56E+03	2624.4
234	3	6.38	6.58	6.63	200	31.4	13.4	8.4	45451	58493	224	1.13E+06	6.16E+03	2173.2
235	4	6.34	6.59	6.65	200	31.4	13.4	8.4	45451	58499	282	1.16E+06	7.95E+03	2723.0
236	1	5.50	5.83	5.91	400	30.5	9.6	9.4	83596	125273	670	2.05E+06	1.75E+04	3550.3
237	2	6.12	6.36	6.42	400	30.5	9.6	9.4	83596	125489	575	2.13E+06	1.54E+04	2624.4
238	3	5.90	6.16	6.22	400	30.5	9.6	9.4	83596	125406	583	2.18E+06	1.61E+04	2825.2
239	4	5.98	6.24	6.31	400	30.5	9.6	9.4	83596	125440	599	2.24E+06	1.70E+04	2831.9
240	1	6.35	6.70	6.78	300	15.0	9.2	9.6	93636	138206	819	3.15E+06	2.87E+04	3765.5
241	2	6.83	7.07	7.13	300	15.0	9.2	9.6	93636	138325	668	3.26E+06	2.61E+04	2624.4
242	3	6.65	6.94	7.01	300	15.0	9.2	9.6	93636	138285	758	3.35E+06	2.81E+04	3151.2
243	4	6.78	7.05	7.12	300	15.0	9.2	9.6	93636	138321	744	3.44E+06	2.83E+04	2940.8
244	1	6.19	6.53	6.61	400	15.5	8.5	9.8	120315	185358	1034	4.01E+06	3.56E+04	3657.9
245	2	6.62	6.87	6.93	400	15.5	8.5	9.8	120315	185502	935	4.15E+06	3.31E+04	2733.8
246	3	6.47	6.77	6.85	400	15.5	8.5	9.8	120315	185462	1054	4.26E+06	3.84E+04	3259.8
247	4	6.59	6.86	6.93	400	15.5	8.5	9.8	120315	185500	1002	4.38E+06	3.75E+04	2940.8
248	1	6.21	6.61	6.71	400	15.2	8.5	9.8	121574	187489	1255	4.10E+06	4.36E+04	4303.4
249	2	6.59	6.84	6.90	400	15.2	8.5	9.8	121538	187517	903	4.23E+06	3.23E+04	2733.8
250	3	6.42	6.74	6.82	400	15.1	8.4	9.8	121792	187902	1113	4.37E+06	4.11E+04	3477.2
251	4	6.53	6.82	6.89	400	15.0	8.5	9.8	122268	188727	1042	4.53E+06	3.96E+04	3158.6
252	1	5.41	5.79	5.88	500	14.9	7.5	10.1	148826	234699	1329	5.08E+06	4.66E+04	4088.3
253	2	5.79	6.03	6.09	500	14.9	7.5	10.1	148826	234815	983	5.25E+06	3.55E+04	2624.4
254	3	5.64	5.96	6.04	500	14.8	7.5	10.1	149321	237620	1251	5.43E+06	4.66E+04	3477.2
255	4	5.76	6.03	6.10	500	14.7	7.5	10.1	149820	238491	1099	5.62E+06	4.22E+04	2940.8
256	1	5.48	5.82	5.90	500	14.9	7.4	10.2	148645	236400	1236	5.08E+06	4.34E+04	3657.9
257	2	5.48	5.82	5.91	500	14.9	7.4	10.2	148645	236404	1262	5.23E+06	4.56E+04	3717.9
258	3	5.69	5.98	6.05	500	14.8	7.4	10.2	149140	237316	1177	5.43E+06	4.38E+04	3151.2
259	4	5.81	6.07	6.14	500	14.7	7.4	10.2	149638	238200	1121	5.62E+06	4.30E+04	2831.9
				Flume bed temperature above 4 degrees C, low flow rates										
216	1	5.05	5.10	5.11	25	29.0	32.3	5.1	9321	(5)	13	1.83E+05	3.48E+02	537.9
217	2	5.99	6.08	6.10	25	29.0	32.3	5.1	9321		24	1.90E+05	6.80E+02	984.2
218	3	6.20	6.23	6.24	25	29.0	32.3	5.1	9321		8	1.96E+05	2.33E+02	326.0
219	4	6.44	6.51	6.53	25	29.0	32.3	5.1	9321		19	2.02E+05	5.65E+02	762.4
220	1	5.04	5.08	5.09	45	31.0	32.0	5.1	15942		11	3.06E+05	2.82E+02	430.3
221	2	6.04	6.13	6.15	45	31.0	32.0	5.1	15942		25	3.19E+05	6.90E+02	984.2
222	3	6.26	6.28	6.29	45	31.0	32.0	5.1	15942		6	3.29E+05	1.58E+02	217.3
223	4	6.43	6.50	6.52	45	31.0	32.0	5.1	15942		20	3.39E+05	5.73E+02	762.4
224	1	7.53	7.65	7.68	75	30.3	31.7	5.1	26836		35	5.37E+05	9.44E+02	1291.0
225	2	8.23	8.33	8.34	75	30.3	31.7	5.1	26836		31	5.58E+05	8.44E+02	1093.5

Entry No.	Station No.	Temperature at (1) (degrees C)	(2)	(3)	Flow Rate (GPM)	Water Depth (cm)	Bulk Temp (C)	Pr no	Hydraulic Diameter Re	Re(4)	Nu	Entrance Length Re	Nu	Heat Flux (W/m^2)
226	3	8.26	8.29	8.30	75	30.3	31.7	5.1	26836		9	5.73E+05	2.59E+02	326.0
227	4	8.34	8.41	8.43	75	30.3	31.7	5.1	26836		21	5.89E+05	6.24E+02	762.4
228	1	5.28	5.48	5.53	100	30.6	32.9	5.0	36443		51	7.01E+05	1.38E+03	2151.7
229	2	6.17	6.31	6.35	100	30.6	32.9	5.0	36443		38	7.29E+05	1.04E+03	1530.9
230	3	6.01	6.07	6.09	100	30.6	32.9	5.0	36443		16	7.47E+05	4.51E+02	652.0
231	4	5.86	5.98	6.01	100	30.6	32.9	5.0	36443		32	7.67E+05	9.27E+02	1307.0
					Flume bed temperature below 4 degrees C, turbulent flow									
70	2	1.78	2.05	2.12	200	13.5	4.8	11.1	57533	78058	541	2.09E+06	2.06E+04	2952.5
71	3	1.55	1.78	1.84	200	13.5	4.8	11.1	57533	77997	415	2.14E+06	1.62E+04	2499.2
72	4	1.57	1.85	1.92	200	13.5	4.8	11.1	57497	77961	524	2.20E+06	2.11E+04	3049.7
73	2	1.73	2.00	2.07	200	13.5	4.8	11.1	57479	77967	537	2.09E+06	2.04E+04	2952.5
74	3	1.50	1.74	1.80	200	13.5	4.8	11.1	57533	77989	427	2.14E+06	1.67E+04	2607.9
75	4	1.54	1.81	1.88	200	13.5	4.9	11.1	57551	78032	493	2.20E+06	1.98E+04	2940.8
76	1	1.12	1.47	1.55	100	15.0	7.8	10.0	29947	35456	315	9.49E+05	1.11E+04	3765.5
77	2	2.06	2.30	2.36	100	15.0	7.8	10.0	29947	35549	252	9.89E+05	9.13E+03	2624.4
78	3	1.74	1.98	2.04	100	15.0	7.8	10.0	29965	35536	236	1.01E+06	8.78E+03	2607.9
79	4	1.55	1.81	1.88	100	15.0	7.8	10.1	29920	35458	251	1.04E+06	9.60E+03	2831.9
80	1	1.02	1.40	1.49	100	15.0	7.8	10.0	29938	35437	339	9.48E+05	1.19E+04	4088.3
81	2	1.96	2.20	2.26	100	15.0	7.8	10.0	29974	35573	246	9.88E+05	8.92E+03	2624.4
82	3	1.70	1.96	2.03	100	15.0	7.8	10.1	29911	35443	257	1.01E+06	9.58E+03	2825.2
83	4	1.50	1.77	1.84	100	15.0	7.8	10.0	29929	35445	258	1.04E+06	9.89E+03	2940.8
84	1	1.72	1.97	2.03	150	14.5	6.3	10.6	43627	56011	325	1.45E+06	1.16E+04	2689.6
85	2	2.45	2.70	2.76	150	14.5	6.3	10.6	43614	56115	400	1.51E+06	1.47E+04	2733.8
86	3	2.28	2.47	2.52	150	14.5	6.3	10.6	43600	56055	283	1.54E+06	1.07E+04	2064.6
87	4	2.26	2.50	2.56	150	14.5	6.3	10.6	43574	56026	365	1.59E+06	1.42E+04	2614.0
88	1	1.64	1.90	1.96	150	14.5	6.3	10.6	43574	55926	336	1.45E+06	1.20E+04	2797.2
89	2	2.35	2.61	2.68	150	14.5	6.2	10.6	43533	55986	413	1.50E+06	1.52E+04	2843.1
90	3.	2.19	2.40	2.45	150	14.5	6.2	10.6	43547	55968	311	1.54E+06	1.18E+04	2281.9
91	4	2.18	2.44	2.51	150	14.5	6.2	10.6	43560	55996	390	1.59E+06	1.51E+04	2831.9
92	1	1.94	2.33	2.42	250	14.0	5.1	11.0	71199	100196	804	2.47E+06	2.92E+04	4195.8
93	2	2.54	2.79	2.85	250	14.0	5.1	11.0	71177	100278	629	2.56E+06	2.35E+04	2733.8
94	3	2.34	2.66	2.74	250	14.0	5.1	11.0	71155	100213	764	2.62E+06	2.93E+04	3477.2
95	4	2.38	2.67	2.74	250	14.0	5.0	11.1	71088	100111	704	2.69E+06	2.78E+04	3158.6
96	1	1.91	2.26	2.34	250	14.0	5.0	11.1	71065	99970	717	2.46E+06	2.60E+04	3765.5
97	2	2.50	2.74	2.80	250	14.0	5.0	11.1	71043	100059	606	2.55E+06	2.26E+04	2624.4
98	3	2.29	2.60	2.68	250	14.0	5.0	11.1	70999	99957	743	2.62E+06	2.85E+04	3368.5
99	4	2.34	2.62	2.69	250	14.0	5.0	11.1	70954	99893	682	2.69E+06	2.69E+04	3049.7
100	1	2.41	2.76	2.84	300	13.7	5.0	11.1	86244	125399	860	3.05E+06	3.16E+04	3765.5
101	2	2.90	3.15	3.21	300	13.7	5.1	11.0	86298	125604	743	3.15E+06	2.81E+04	2733.8
102	3	2.70	3.01	3.09	300	13.7	5.1	11.0	86379	125691	844	3.24E+06	3.28E+04	3368.5
103	4	2.75	3.03	3.10	300	13.6	5.1	11.0	86760	126318	755	3.35E+06	3.02E+04	3049.7
104	1	2.58	2.94	3.03	300	13.7	5.2	11.0	86569	125970	910	3.06E+06	3.34E+04	3873.1
105	2	3.07	3.33	3.40	300	13.7	5.2	11.0	86623	126175	800	3.17E+06	3.02E+04	2843.1
106	3	2.86	3.18	3.26	300	13.7	5.2	11.0	86677	126216	899	3.25E+06	3.49E+04	3477.2
107	4	2.91	3.20	3.27	300	13.6	5.2	11.0	87060	126846	806	3.37E+06	3.23E+04	3158.6
108	1	0.65	1.06	1.16	120	15.0	6.4	10.5	34410	42028	443	1.11E+06	1.56E+04	4411.0
109	2	1.48	1.71	1.77	120	15.0	6.3	10.6	34378	42066	288	1.15E+06	1.04E+04	2515.1
110	3	1.22	1.51	1.58	120	15.0	6.3	10.6	34314	41956	351	1.18E+06	1.31E+04	3151.2
111	4	1.17	1.45	1.52	120	15.0	6.3	10.6	34306	41933	336	1.21E+06	1.28E+04	3049.7
112	1	0.55	0.92	1.01	120	15.0	6.3	10.6	34293	41851	397	1.10E+06	1.40E+04	3980.7
113	2	1.36	1.58	1.64	120	15.0	6.2	10.6	34219	41834	277	1.14E+06	1.00E+04	2405.7
114	3	1.13	1.40	1.47	120	15.0	6.2	10.6	34229	41826	325	1.17E+06	1.21E+04	2933.9
115(6)	4	1.08	1.35	1.42	120	15.0	6.1	10.6	34155	41720	327	1.20E+06	1.25E+04	2940.8
120	1	1.07	1.38	1.45	100	15.0	8.2	9.9	30274	35874	259	9.53E+05	9.14E+03	3335.2
121	2	1.99	2.24	2.30	100	15.0	8.1	9.9	30256	35949	244	9.94E+05	8.86E+03	2733.8
122	3	1.75	1.97	2.03	100	15.0	8.1	9.9	30267	35904	204	1.02E+06	7.61E+03	2390.6
123	4	1.61	1.87	1.94	100	15.0	8.1	9.9	30238	35882	239	1.04E+06	9.14E+03	2831.9
124	1	1.07	1.44	1.53	100	15.0	8.1	9.9	30265	35871	313	9.54E+05	1.10E+04	3980.7
125	2	1.97	2.23	2.30	100	15.0	8.1	9.9	30265	35960	253	9.94E+05	9.18E+03	2843.1
126	3	1.74	1.96	2.02	100	15.0	8.1	9.9	30229	35879	205	1.02E+06	7.62E+03	2390.6
127	4	1.62	1.88	1.95	100	15.0	8.1	9.9	30238	35883	239	1.04E+06	9.16E+03	2831.9

Entry No.	Station No.	Temperature at (1) (degrees C)	ī (2)	(3)	Flow Rate (GPM)	Water Depth (cm)	Bulk Temp (C)	Pr no	Hydraulic Diameter Re	Re(4)	Nu	Entrance Length Re	Nu	Heat Flux (W/m^2)
128	1	0.31	0.68	0.77	80	15.2	8.6	9.8	24351	27437	268	7.49E+05	9.39E+03	3980.7
129	2	1.33	1.57	1.63	80	15.2	8.6	9.8	24351	27318	199	7.81E+05	7.16E+03	2624.6
130	3	0.95	1.19	1.25	80	15.2	8.6	9.8	24373	27310	186	7.99E+05	6.91E+03	2607.9
131	4	0.72	0.97	1.03	80	15.2	8.6	9.8	24373	27489	189	8.18E+05	7.20E+03	2723.0
132	1	0.20	0.60	0.70	80	15.2	8.6	9.8	24373	27458	286	7.48E+05	1.00E+04	4303.6
133	2	1.20	1.43	1.49	80	15.2	8.5	9.8	24322	27468	188	7.79E+05	6.76E+03	2515.1
134	3	0.90	1.14	1.20	80	15.2	8.6	9.8	24351	27478	186	7.98E+05	6.89E+03	2607.9
135	4	0.67	0.94	1.01	80	15.2	8.5	9.8	24337	27441	205	8.17E+05	7.80E+03	2940.8
136	1	1.73	2.08	2.16	60	14.5	10.8	9.1	19944	21550	223	6.23E+05	8.01E+03	3765.5
137	2	2.77	3.04	3.11	60	14.5	10.7	9.1	19938	21613	196	6.50E+05	7.26E+03	2952.5
138	3	2.54	2.77	2.83	60	14.5	10.9	9.1	20013	21683	158	6.67E+05	6.00E+03	2499.2
139	4	2.29	2.56	2.63	60	14.5	10.9	9.0	20062	21703	180	6.83E+05	7.03E+03	2940.8
140	1	1.04	1.45	1.55	60	14.5	10.5	9.2	19806	21338	250	6.14E+05	9.00E+03	4411.0
141	2	2.00	2.24	2.30	60	14.5	10.6	9.2	19829	21421	162	6.40E+05	5.98E+03	2624.6
142	3	1.70	1.89	1.94	60	14.5	10.5	9.2	19789	21346	123	6.54E+05	4.67E+03	2066.6
143	4	1.31	1.54	1.60	60	14.5	10.5	9.2	19783	21314	143	6.68E+05	5.61E+03	2505.1
144	1	0.68	1.04	1.13	60	14.3	10.5	9.2	19934	21505	208	6.19E+05	7.56E+03	3873.1
145	2	1.99	2.26	2.33	60	14.3	10.5	9.2	19934	21594	182	6.49E+05	6.79E+03	2952.5
146	3	1.71	1.91	1.96	60	14.3	10.5	9.2	19934	21566	128	6.63E+05	4.92E+03	2173.2
147	4	1.05	1.31	1.38	60	14.3	10.5	9.2	19946	21537	156	6.75E+05	6.15E+03	2831.9
148	1	0.60	0.93	1.01	60	14.3	10.5	9.2	19940	21503	188	6.18E+05	6.84E+03	3550.3
149	2	1.95	2.19	2.25	60	14.3	10.5	9.2	19923	21574	161	6.48E+05	6.00E+03	2624.4
150	3	1.59	1.76	1.80	60	14.3	10.5	9.2	19911	21527	108	6.61E+05	4.13E+03	1847.2
151	4	1.05	1.30	1.36	60	14.3	10.5	9.2	19928	21515	150	6.75E+05	5.93E+03	2723.0
152	1	0.52	0.95	1.05	60	14.3	10.3	9.2	19807	21346	253	6.16E+05	9.18E+03	4626.2
153	2	1.57	1.82	1.88	60	14.3	10.3	9.2	19813	21414	164	6.43E+05	6.12E+03	2733.8
154	3	1.09	1.28	1.33	60	14.3	10.3	9.2	19819	21380	116	6.55E+05	4.45E+03	2064.6
155	4	0.60	0.86	0.93	60	14.3	10.2	9.2	19784	21309	153	6.68E+05	6.05E+03	2831.9
156	1	0.51	0.95	1.05	60	14.3	10.3	9.2	19813	21353	259	6.16E+05	9.38E+03	4733.8
157	2	1.59	1.84	1.90	60	14.3	10.2	9.3	19764	21332	167	6.42E+05	6.22E+03	2733.8
158	3	1.11	1.29	1.33	60	14.3	10.2	9.3	19761	21311	111	6.54E+05	4.27E+03	1955.9
159	4	0.69	0.94	1.00	60	14.3	10.3	9.2	19796	21328	148	6.69E+05	5.85E+03	2723.0
160	1	1.06	1.38	1.46	72	14.0	7.5	10.1	22131	24719	285	7.28E+05	1.04E+04	3442.7
161	2	1.87	2.04	2.08	72	14.0	7.5	10.1	22097	24730	173	7.54E+05	6.50E+03	1859.0
162	3	1.72	1.86	1.89	72	14.0	7.5	10.1	22117	24739	136	7.75E+05	5.25E+03	1521.3
163	4	1.51	1.71	1.76	72	14.0	7.5	10.1	22126	24736	190	7.95E+05	7.54E+03	2178.4
164	1	0.94	1.17	1.22	72	14.0	7.6	10.1	22138	24708	197	7.25E+05	7.19E+03	2474.5
165	2	1.85	2.05	2.10	72	14.0	7.5	10.1	22131	24773	202	7.57E+05	7.60E+03	2187.0
166	3	1.64	1.82	1.87	72	14.0	7.5	10.1	22104	24720	175	7.75E+05	6.74E+03	1955.9
167	4	1.56	1.81	1.87	72	14.0	7.5	10.1	22117	24737	243	7.96E+05	9.62E+03	2723.0
168	1	·0.68	0.91	0.96	72	14.0	7.1	10.3	21816	24289	204	7.17E+05	7.46E+03	2474.5
169	2	1.49	1.69	1.74	72	14.0	7.0	10.3	21796	24328	208	7.47E+05	7.81E+03	2187.0
170	3	1.31	1.45	1.49	72	14.0	7.0	10.3	21763	24266	139	7.64E+05	5.38E+03	1521.3
171	4	1.10	1.29	1.34	72	14.0	6.9	10.3	21723	24204	187	7.82E+05	7.40E+03	2069.5
172	1	0.66	0.90	0.96	72	14.0	7.0	10.3	21749	24206	217	7.16E+05	7.90E+03	2582.1
173	2	1.51	1.71	1.76	72	14.0	7.0	10.3	21763	24288	211	7.46E+05	7.91E+03	2187.0
174	3	1.28	1.44	1.48	72	14.0	6.9	10.3	21723	24216	161	7.63E+05	6.21E+03	1738.6
175	4	1.07	1.28	1.33	72	14.0	6.9	10.3	21716	24195	206	7.82E+05	8.18E+03	2287.3
176	1	0.15	0.46	0.53	57	14.0	8.0	10.0	17788	18851	223	5.72E+05	8.17E+03	3335.2
177	2	1.06	1.26	1.31	57	14.0	8.2	9.9	17890	19025	159	5.98E+05	5.97E+03	2187.0
178	3	0.67	0.81	0.85	57	14.0	8.2	9.9	17863	18961	104	6.10E+05	4.03E+03	1521.3
179	4	0.29	0.51	0.57	57	14.0	8.1	9.9	17804	18873	160	6.23E+05	6.38E+03	2396.2
180	1	-0.02	0.27	0.34	57	14.0	8.3	9.9	17917	18991	197	5.73E+05	7.22E+03	3120.0
181	2	0.90	1.11	1.16	57	14.0	8.3	9.9	17906	19034	163	5.97E+05	6.12E+03	2296.4
182	3	0.52	0.65	0.68	57	14.0	8.2	9.9	17868	18957	95	6.09E+05	3.66E+03	1612.6
183	4	0.14	0.32	0.37	57	14.0	8.2	9.9	17895	18968	125	6.22E+05	4.97E+03	1960.5
					Flume bed temperature below 4 degrees C, low flow rates									
184	1	1.64	1.73	1.75	45	25.5	21.1	6.7	14314	(5)	32	3.08E+05	9.02E+02	968.3
185	2	2.12	2.19	2.21	45	25.5	21.1	6.7	14317		26	3.19E+05	7.51E+02	765.5
186	3	2.03	2.06	2.07	45	25.5	21.1	6.7	14321		11	3.27E+05	3.26E+02	326.0
187	4	1.81	1.86	1.87	45	25.5	21.1	6.7	14321		18	3.35E+05	5.54E+02	544.6

Entry No.	Station No.	Temperature at (1) (degrees C)	(2)	(3)	Flow Rate (GPM)	Water Depth (cm)	Bulk Temp (C)	Pr no	Hydraulic Diameter Re	Re(4)	Nu	Entrance Length Re	Nu	Heat Flux (W/m^2)
188	1	0.05	0.11	0.12	45	27.9	33.0	5.0	17444		12	3.24E+05	3.48E+02	645.5
189	2	1.11	1.20	1.22	45	27.9	33.0	5.0	17447		20	3.38E+05	5.64E+02	984.2
190	3	1.22	1.24	1.25	45	27.9	33.0	5.0	17454		4	3.48E+05	1.28E+02	217.3
191	4	0.88	0.95	0.97	45	27.9	33.0	5.0	17454		15	3.56E+05	4.57E+02	762.4
192	1	0.15	0.22	0.24	45	27.9	33.0	5.0	17458		15	3.24E+05	4.07E+02	753.1
193	2	1.23	1.33	1.36	45	27.9	33.0	5.0	17458		22	3.39E+05	6.29E+02	1093.5
194	3	1.34	1.36	1.37	45	27.9	33.0	5.0	17461		4	3.48E+05	1.28E+02	217.3
195	4	0.97	1.04	1.06	45	27.9	33.0	5.0	17461		15	3.56E+05	4.58E+02	762.4
196	1	1.56	1.62	1.63	35	30.3	30.2	5.3	12148		15	2.28E+05	4.01E+02	645.5
197	2	2.58	2.67	2.69	35	30.3	30.2	5.3	12148		23	2.38E+05	6.53E+02	984.2
198	3	2.78	2.81	2.82	35	30.3	30.2	5.3	12148		8	2.45E+05	2.23E+02	326.0
199	4	2.79	2.85	2.87	35	30.3	30.2	5.3	12148		16	2.52E+05	4.60E+02	653.5
200	1	0.88	0.92	0.93	10	29.0	32.0	5.1	3706		9	6.90E+04	2.45E+02	430.3
201	2	1.88	1.97	1.99	10	29.0	32.0	5.1	3706		21	7.20E+04	5.97E+02	984.2
202	3	2.08	2.10	2.11	10	29.0	32.0	5.1	3706		5	7.42E+04	1.36E+02	217.3
203	4	2.24	2.30	2.32	10	29.0	32.0	5.1	3706		14	7.64E+04	4.23E+02	653.5
204	1	0.83	0.88	0.89	10	29.0	32.1	5.1	3712		11	6.91E+04	2.93E+02	516.4
205	2	1.88	1.97	1.99	10	29.0	32.1	5.1	3712		20	7.21E+04	5.62E+02	929.5
206	3	2.08	2.09	2.10	10	29.0	32.1	5.1	3712		4	7.42E+04	1.22E+02	195.6
207	4	2.22	2.28	2.30	10	29.0	32.1	5.1	3712		16	7.64E+04	4.64E+02	718.9
208	1	0.84	0.88	0.89	10	29.0	32.2	5.1	3718		10	6.91E+04	2.68E+02	473.4
209	2	1.89	1.98	2.00	10	29.0	32.2	5.1	3718		21	7.22E+04	5.94E+02	984.2
210	3	2.09	2.11	2.11	10	29.0	32.2	5.1	3718		4	7.43E+04	1.29E+02	206.5
211	4	2.26	2.31	2.33	10	29.0	32.2	5.1	3718		16	7.65E+04	4.70E+02	729.8
212	1	1.05	1.11	1.12	25	30.5	33.1	5.0	9168		13	1.67E+05	3.57E+02	645.5
213	2	2.15	2.24	2.26	25	30.5	33.1	5.0	9168		21	1.74E+05	5.79E+02	984.2
214	3	2.37	2.39	2.40	25	30.5	33.1	5.0	9168		5	1.79E+05	1.32E+02	217.3
215	4	2.51	2.58	2.60	25	30.5	33.1	5.0	9168		16	1.85E+05	4.79E+02	762.4

APPENDIX D: ERROR ANALYSIS

NUSSELT NUMBER

In order to conduct an error analysis of the Nusselt number, an accuracy value for each measured or calculated value had to be determined. The Nusselt number was calculated from

$$\mathrm{Nu}_H = \frac{h\,D_H}{K} \tag{D1}$$

where

$$h = \frac{K_{AL}(\Delta T_{AL})}{L\,(\Delta T_w)} \tag{D2}$$

$$D_H = \frac{4d\,(0.3048)}{(2d + 0.3048\,)} \tag{D3}$$

K_{AL}	=	conductivity of aluminum	$\pm$ 13.8 W/m°K
ΔT_{AL}	=	temperature difference between thermistors in the plate	$\pm$ 0.028°C
L	=	distance between thermistors in the plate	$\pm$ 0.001 m
ΔT_W	=	bed surface temperature—bulk water temperature	$\pm$ 0.045°C
d	=	water depth	$\pm$ 0.001 m
K	=	conductivity of the water at the bulk temperature	nil

REYNOLDS NUMBER

Describing the Reynolds number calculations similarly,

$$\mathrm{Re}_H = \frac{V\,D_H}{\nu} \tag{D4}$$

where

V	=	QA	
Q	=	volumetric flow rate	$\pm 3.14 \times 10^{-4}\,\mathrm{m^3/s}$
A	=	cross section area	nil
ν	=	dynamic viscosity at bulk temperature	nil
D_H	=	eq D3.	

Using the equation for uncertainty (Holman 1971)

$$W_r = \left[\left(\frac{\partial R}{\partial x_1} W_1\right)^2 + \left(\frac{\partial R}{\partial x_2} W_2\right)^2 + \left(\frac{\partial R}{\partial x_3} W_3\right)^2 + \ldots\right]^{1/2}. \tag{D5}$$

where R is the function, $x_1, x_2, x_3 \ldots x_n$ are the independent variables, and $W_1, W_2, W_3 \ldots W_r$ are the uncertainties of the independent variables. The following were calculated for two typical entries 206 (low flow rate) and 248 (high flow rate).

	Uncertainty			
	Entry 206		*Entry 248*	
h	± 10.2	± 157%	± 353	± 15%
Nu_H	± 6.5	± 160%	± 186	± 15%
V	± 0.0035	± 50%	± 0.0075	± 1%
Re_H	± 1847	± 50%	± 1513	± 1%

APPENDIX E: DATA ANALYSIS PROGRAM

```
'ANALYSIS OF FLUME DATA
        DEFDBL B,D
        DIM S(300),T1(300),T2(300),F(300),D(300),B(300)
'READ DATA FILE
        OPEN "FDATA" FOR INPUT AS #1
        INPUT #1 , N
        FOR I=1 TO N
        INPUT #1, S(I),T1(I),T2(I),F(I),D(I),B(I)
        NEXT I
        CLOSE
'*********************************************************************
500     PRINT "PRINT DATA=1"
        PRINT "ANALYSIS OF ALL DATA =2"
        PRINT "RECALCULATE INDIVIDUAL DATA SET =3"
        PRINT "EXIT=4"
        INPUT "SELECT OPTION";S1
        IF S1=4 THEN STOP
        IF S1=3 THEN GOTO 660
        IF S1=2 THEN J=1:J1=N: GOSUB 710
        IF S1<>1 THEN GOTO 500
'*********************************************************************
590     LPRINT SPC(13) "ENTRY  STATION  TEMPERATURE  FLOW  DEPTH  BULK"
        LPRINT SPC(15) "NO.    NO.     @ .325   @ 1.59  GPM   CM     TEMP"
            LPRINT
            FOR I=1 TO N
        LPRINT USING "        ###";I;
        LPRINT USING "     #";S(I);
        LPRINT USING "     #.##";T1(I);
        LPRINT USING "     #.##";T2(I);
        LPRINT USING "     ###";F(I);
        LPRINT USING "     ##.##";D(I);
        LPRINT USING "     ##.##";B(I)
        NEXT I
650     GO TO 500
'*********************************************************************
660     J3=0               'RECALCULATES INDIVIDUAL OR GROUPS OF DATA
670     INPUT "ENTER FIRST DATA SET NUMBER"; J
        INPUT "ENTER LAST DATA SET NUMBER"; J1
        GOSUB 710
        GOTO 500
'*********************************************************************
710     'SUBROUTINE TO CALCULATE EXPERIMENTAL PARAMETERS

'VISC OF WATER
        DEF FNV(T)=(-(4.375E-06*T^3)+.0013*T^2-.1488*T+7.9)*4.1339E-04
'COND. OF WATER
```

```
        DEF FNK(T)=(-(1.11E-06*T^2)+.0006889*T+.306)*1.7303
'PR. NO.
        DEF FNP(T)=-(1.563E-05*T^3)+.004625*T^2-.5178*T+25.6
'DENSITY OF WATER
        DEF FND2(T)=(999.83952#+16.945176#*T-.0079870401#*T^2-.000046170461#*T^3+
.00000010556302*T^4-2.8054253D-10*T^5)/(1+.01687985#*T)

'ENTRANCE LENGTH TO EACH STATION
        L1(1)=10.55
        L1(2)=10.86
        L1(3)=11.164
        L1(4)=11.465
'DISTANCE BETWEEN THERMISTORS AT EACH STATION
        L2(1)=.012827
        L2(2)=.01262
        L2(3)=.0127
        L2(4)=.01267
        K1=138          'CONDUCTIVITY OF FLUME BED  W/M DEG C

PRINT DATA TO A TEXT FILE
        INPUT "WRITE FLOW CHARACTERISTICS TO A FILE";FI$
        IF FI$="Y" OR FI$="Y" THEN
CHANGE THE NAME OF THE OUTPUT FILE HERE
        OPEN "ADATA.DAT" FOR OUTPUT AS #2
        END IF

        INPUT "REGRESSION ANALYSIS (Y/N)";CAL$

1220    FOR I=J TO J1
        IF I>=116 AND I<=119 THEN GOTO 1300SKIPS UNSTEADY DATA
        J3=J3+1
        HF=K1*(T1(I)-T2(I))/L2(S(I))            'HEAT FLUX
        B1=B(I)*1.8+32                          'BULK TEMP IN DEG F
        'SURFACE TEMPERATURE
        T3=(T2(I)-T1(I))*(0.01905-L2(S(I))-0.003175)/L2(S(I))+T2(I)
        B2=T3*1.8+32                            'SURFACE TEMP IN DEG F
        B3=(B1+B2)/2                            'FILM TEMP IN DEG F
        B9=(B3-32)/1.8                          'FILM TEMP IN DEG C

PROPERTIES BASED ON FILM TEMPERATURE
        B4=FND2(B9)                             'DENSITY OF WATER  KG/M^3
        B8=FNV(B3)/B4                           'DYNAMIC VISCOSITY  M^2/S (FILM TEMP)
        B5=FNK(B3)                              'CONDUCTIVITY OF WATER   W/M^2
        B7=FNP(B3)                              'PR NO.

PROPERTIES BASED ON BULK TEMPERATURE
        B4B=FND2(B(I))                          'DENSITY OF WATER
        B8B=FNV(B1)/B4B                         'DYNAMIC VISCOSITY
        B5B=FNK(B1)                             'CONDUCTIVITY OF WATER
        B7B=FNP(B1)                             'PR. NO.
```

```
        H=HF/(T3-B(I))                          'HEAT TRANSFER COEFF
        FM=F(I)*6.30902E-05                     'MASS FLOW IN M^3/S
        F=FM/(30.4*D(I)/10000)                  'FLOW VELOCITY IN M/S
        H9=4*30.48*D(I)/(2*D(I)+30.48)/100      'HYDRAULIC DIAM (M)
        R5=F*H9/B8B                             'RE NO. HYD DIAM
        R6=F*L1(S(I))/B8                        'RE NO. ENTRANCE LENGTH
        N1=H*H9/B5B                             'NU.NO. HYD DIAM
        N2=H*L1(S(I))/B5                        'NU NO. ENTRANCE LENGTH

        GOSUB VELOCITY              'VELOCITY CORRECTION
        RHV=F*H9/B8B                'RE .NO. HYD DIAM W/VELOCITY CORRECTION

'ADJUST FOLLOWING PRINT STATEMENTS TO GET DESIRED OUTPUT FILE
        IF FI$="Y" OR FI$="Y" THEN
        PRINT #2, USING "                     ###";I;
        PRINT #2, USING "        #";S(I);
        PRINT #2, USING "     #.##";T1(I);
        PRINT #2, USING "     #.##";T2(I);
        PRINT #2, USING "      ###";F(I);
        PRINT #2, USING "    ##.##";D(I);
        PRINT #2, USING "    ##.##";B(I);
        PRINT #2, USING "   ###.##";B7B;
        PRINT #2, USING "   ######";R5;
        PRINT #2, USING "  ######";RHV;
        PRINT #2, USING "     ####";N1;
        PRINT #2, USING "   #.##^^^^";R6;
        PRINT #2, USING "   #.##^^^^";N2;
        PRINT #2, USING "  ####.##";-HF
        END IF

        IF CAL$="Y" OR CAL$="Y" THEN
        'REGRESSION ANALYSIS
        Y1=N1/(B7B^(1/3))                 'SETS Y OF REGRESSION ANALYSIS
        X1=R5                             'SETS X OF REGRESSION ANALYSIS
        DMAT(2,1)=LOG(X1)+DMAT(2,1)
        DMAT(1,2)=DMAT(2,1)
        DMAT(2,2)=(LOG(X1)^2)+DMAT(2,2)
        RMAT(1)=LOG(Y1)+RMAT(1)
        RMAT(2)=LOG(Y1)*LOG(X1)+RMAT(2)
        END IF

        PRSUM=PRSUM+B7B

1300    NEXT I

        DMAT(1,1)=J3
        INPUT "MORE DATA (Y/N)";Y$
        IF Y$="Y" OR Y$="Y" THEN
        GOTO 670
        PRINT "PR AVG=";PRSUM/J3
        ELSE
```

```
       IF CAL$="Y" OR CAL$="Y" THEN GOSUB GAUSS
       END IF
       PRINT "PR AVG=";PRSUM/J3                    'CALCULATES AVG PRANDTL NO.
1350   RETURN

GAUSS:              'SUBROUTINE GAUSS-SIEDEL METHOD MATRIX SOLVER
       W=1.8
       XMAT(1)=1      :XMAT(2)=1
       P=1
       SE=0
1375   M=0
       FOR I=1 TO 2
       TM=RMAT(I)
       FOR I1=1 TO 2
       IF I=I1 THEN 1400
       TM=TM-XMAT(I1)*DMAT(I,I1)
1400   NEXT I1
       TM=TM/DMAT(I,I)
       EM=TM-XMAT(I)
       SE=SE+(XMAT(I)/TM)^2
       IF ABS(EM)<.000001 THEN 1460
       M=M+1
1460   XMAT(I)=XMAT(I)+W*(TM-XMAT(I))
       NEXT I
       IF P=1 THEN 1500
'CALCULATE SPECTRAL RADIUS
       SD=SQR(S1/SE)
       PRINT "SPECTRAL RADIUS ESTIMATE ";SD
1500       S1=SE
       IF M=0 OR P=2500 THEN 1580
       SE=0
       P=P+1
       GOTO 1375
1580   PRINT EXP(XMAT(1))
       PRINT XMAT(2)
       PRINT "NUMBER OF ITERATIONS REQUIRED WAS ";P
       RETURN

VELOCITY:           'CORRECTION
       NN=.012                                'MANNING'S COEFF.
       FF=F/.3048                             'VELOCITY IN FT/S
       RT=H9/.3048/4                          'HYDRAULIC RADIUS
       FT=8*32.17*(NN/1.49)^2*RT^(-1/3)
       REF=(F*H9/B8)/FT                       'RE(H)/F
       FW=.2526414*REF^-.16912927#            'CURVE FIT
       FB=FT+(2*D(I)/30.48)*(FT-FW)
       UB=SQR(FB*F^2/8)
       REB=(UB*D(I)/100)/B8
       F=UB*(2.5*LOG(3.32*REB))
       RETURN
       END
```

REPORT DOCUMENTATION PAGE

Form Approved
OMB No. 0704-0188

1. AGENCY USE ONLY (Leave blank)	2. REPORT DATE	3. REPORT TYPE AND DATES COVERED
	May 1990	

4. TITLE AND SUBTITLE

Heat Transfer From Water Flowing Through a Chilled-Bed Open Channel

5. FUNDING NUMBERS

PE: 7.627.30A
PR: 4A762730A4AL
WU: ILIR

6. AUTHORS

Richmond, Paul W. and Lunardini, Virgil J.

7. PERFORMING ORGANIZATION NAME(S) AND ADDRESS(ES)

U.S. Army Cold Regions Research and Engineering Laboratory
72 Lyme Road
Hanover, New Hampshire 03755-1290

8. PERFORMING ORGANIZATION REPORT NUMBER

CRREL Report 90-3

9. SPONSORING/MONITORING AGENCY NAME(S) AND ADDRESS(ES)

Office of the Chief of Engineers
Washington, DC 20314-1000

10. SPONSORING/MONITORING AGENCY REPORT NUMBER

11. SUPPLEMENTARY NOTES

12a. DISTRIBUTION/AVAILABILITY STATEMENT

Approved for public release; distribution is unlimited.

Available from NTIS, Springfield, Virginia 22161

12b. DISTRIBUTION CODE

13. ABSTRACT (*Maximum 200 words*)

Observations and experiments have shown that heat transfer is greater for water flowing over ice than for water flowing over flat plates without melting. The mechanisms that contribute to this increased heat transfer are not completely understood. One possible cause is the density inversion of water at 4°C. In order to investigate this effect on heat transfer, a small open-channel flume was designed and constructed. Experiments were conducted with the flume bed at temperatures slightly above 0°C and at temperatures above 4°C. Bulk water temperatures ranged from 5° to 33°C. Flow data were obtained for $2.5 \times 10^3 < Re_H < 10^5$. At high flow rates (fully developed turbulent flow) heat transfer correlations were determined and compared with other correlations. The correlations obtained from these experiments initially showed higher heat transfer rates than those obtained from experiments in larger flumes with ice present. This is thought to be due to a difference in velocity profiles caused by the flume width. Once velocity corrections were made to the data, they agreed more closely with experiments from wider flumes. The results indicate that the density inversion of water could account for most of the increased turbulent heat transfer observed between melting and nonmelting systems. The heat transfer data at low flow rates are more qualitative than quantitative due to difficulty in obtaining accurate data.

14. SUBJECT TERMS

Freshwater ice	Ice covers
Heat transfer	Water flows

15. NUMBER OF PAGES 56

16. PRICE CODE

17. SECURITY CLASSIFICATION OF REPORT	18. SECURITY CLASSIFICATION OF THIS PAGE	19. SECURITY CLASSIFICATION OF ABSTRACT	20. LIMITATION OF ABSTRACT
UNCLASSIFIED	UNCLASSIFIED	UNCLASSIFIED	UL

NSN 7540-01-280-5500

☆ U. S. GOVERNMENT PRINTING OFFICE: 1990--700-057--22014

Standard Form 298 (Rev. 2-89)
Prescribed by ANSI Std. Z39-18
298-102